

Hyperfine structure of the $A^1\Pi$ state of AlCl and its relevance to laser cooling and trapping

John R. Daniel,^{1,*} Jamie C. Shaw,^{2,*} Chen Wang,¹ Li-Ren Liu,¹
Brian K. Kendrick,³ Boerge Hemmerling,^{1,†} and Daniel J. McCarron^{2,‡}

¹*Department of Physics and Astronomy, University of California, Riverside, California 92521, USA*

²*Department of Physics, University of Connecticut,*

196A Auditorium Road, Unit 3046, Storrs, CT 06269-3046

³*Theoretical Division (T-1, MS B221), Los Alamos National Laboratory, Los Alamos, New Mexico 87545, USA*

(Dated: October 2, 2023)

The majority of molecules proposed for laser cooling and trapping experiments have Σ -type ground states. Specifically, $^2\Sigma$ states have cycling transitions analogous to D1-lines in alkali atoms while $^1\Sigma$ states offer both strong and weak cycling transitions analogous to those in alkaline earth atoms. Despite this proposed variety, to date, only molecules with $^2\Sigma$ -type ground states have successfully been confined and cooled in magneto-optical traps. While none of the proposed $^1\Sigma$ -type molecules have been successfully laser cooled and trapped, they are expected to have various advantages in terms of exhibiting a lower chemical reactivity and an internal structure that benefits the cooling schemes. Here, we present the prospects and strategies for optical cycling in AlCl – a $^1\Sigma$ molecule – and report on the first characterization of the $A^1\Pi$ state hyperfine structure. Based on these results, we carry out detailed simulations on the expected capture velocity of a magneto-optical trap for AlCl. Finally, using *ab initio* calculations, we identify the two-photon photo-ionization process via the $3^1\Sigma^+$ state as a possible loss mechanism for a MOT of AlCl.

I. INTRODUCTION

The ability to control the rich internal and external degrees of freedom of polar molecules has the prospect of enabling a large number of novel applications, including the search for new physics beyond the Standard Model and precision measurements [1–21], controlled chemistry [22–25], and quantum simulation and computation [26–32]. Realizing the necessary control for such applications can realistically only be achieved at low temperatures, where only a small number of quantum states are occupied, and with trapped samples that allow for long interaction times. One way to produce ultracold molecules is to associate laser cooled atoms with carefully controlled external fields. While this method has been successful, it is limited to molecules which consist of laser coolable atoms [33–42]. On the other hand, over the past two decades, a growing number of molecules have been identified with internal structures that allow for photon cycling to an extent that renders these molecules amenable to direct laser cooling and trapping [43–48]. Among those species, a diverse range of diatomic molecules have been explored both theoretically [49–64] and experimentally [49, 65–86]. Furthermore, this experience has helped to guide recent efforts extending these techniques to polyatomic species [3, 87–96].

Nevertheless, at present, only the diatomic molecules SrF [97, 98], CaF [99–101], YO [102] and the polyatomic CaOH [93] have successfully been laser cooled and con-

fined in a magneto-optical trap (MOT), a crucial milestone towards the growing list of applications. All of these molecules possess an unpaired electronic spin and a $^2\Sigma$ -type ground state with optical cycling transitions analogous to D1 lines in alkali atoms. By contrast, molecules with $^1\Sigma$ ground states are expected to offer certain advantages for laser cooling, as their closed shells render them less reactive and their internal structures show similarities to atoms in a type-II MOT. For $^1\Sigma$ molecules, both strong and weak optical cycling transitions may be available, analogous to the $^1S_0 \rightarrow ^1P_1$ and $^1S_0 \rightarrow ^3P_J$ transitions regularly used in alkaline earth atoms. To the best of our knowledge, the only three $^1\Sigma$ -type species currently being experimentally studied for laser cooling are TlF [67, 103, 104], AlF [82, 83] and AlCl [43, 56, 105, 106].

In this work, we spectroscopically study the hyperfine and the magnetic sub-structure of AlCl, discuss the implications of its properties on laser cooling and trapping and present theoretical estimates of the expected capture velocities of a MOT for AlCl. The metal halide AlCl has been proposed as an excellent candidate for laser cooling due to its high photon scattering rate of $\approx 2\pi \times 25$ MHz [107] and its almost unity Franck-Condon factors [56, 105, 106, 108, 109]. A key challenge to laser cooling and trapping AlCl is producing sufficient laser light for the optical cycling transition at 261.5 nm which connects the electronic ground $X^1\Sigma^+$ state with the excited $A^1\Pi$ state. However, recent developments in UV laser technology, including work done by the authors, have shown that robust systems capable of more than 1 W of laser power at this wavelength are now within reach [110–114].

AlCl was first laboratory-confirmed in 1913 and has since undergone many spectroscopic and chemical stud-

* These two authors contributed equally.

† boergeh@ucr.edu

‡ daniel.mccarron@uconn.edu

ies [106, 107, 115–143]. Moreover, these efforts have been complemented by many theoretical studies that explored the properties of AlCl in detail [56, 105, 106, 108, 109, 144–152]. Its presence in the interstellar medium, carbon-rich stars, and as part of the models of exoplanets’ atmospheres renders AlCl a molecule of astrophysical interest [145, 146, 148, 153–161]. Despite this extensive work, some fundamental properties, such as the dipole moment of AlCl, remain unknown and have only been estimated theoretically [146] or in some models substitute values from similar molecules are used [154, 155]. AlCl also has many applications outside the laboratory, for instance, it is utilized in the production of photovoltaic grade silicon [162–164], is spectroscopically found in rocket plumes [165–167] and can be used as a probe for the detection of chlorides in drinking water [168]. Another interesting and unique aspect of AlCl is that the disproportionation reaction channel, which forms the stable compound AlCl_3 , can be blocked below 180 K and solid densities of AlCl have been isolated using this characteristic [169]. This property can potentially provide the ideal starting point for producing a large number of molecules in the gas phase by applying nanosecond-pulsed laser ablation to a fabricated thin precursor film of AlCl, adding to the list of advantages of AlCl as a candidate for laser cooling and trapping and the described applications.

II. THE ALCL STRUCTURE

AlCl has two main isotopes with $^{35,37}\text{Cl}$ with natural abundances of $\approx 76\%$ and $\approx 24\%$ respectively. The large differences in the electronegativities between Al (1.61) and Cl (3.16) form a polar bond with a theoretically predicted electric dipole moment of 1.6 D for the $X^1\Sigma^+$ state [146]. The $X^1\Sigma^+$ ground state is connected via a UV photon at 261.5 nm to the excited, short-lived $A^1\Pi$ state, which has a lifetime of ≈ 6 ns [107], and via a blue photon at ≈ 407 nm to the intermediate triplet $a^3\Pi$ state. The meta-stable intermediate state is split into four Ω -sub states whose linewidths have been estimated to be on the order of 3–90 Hz [105], but no precise experimental data exists to date. The $A^1\Pi \leftarrow X^1\Sigma^+$ excitation, which promotes a valence electron from the 9σ - to the 4π -orbital, closely resembles the S-P transition in atomic aluminum [132]. The similar vibrational constants and bond lengths of the $X^1\Sigma^+$ and the $A^1\Pi$ states result in a calculated Franck-Condon factor of 99.88% for the $v'' = 0$ band [106]. The vibrational levels are split in rotational states with a rotational constant of ≈ 7.3 GHz. The presence of the nuclear spins of both the chlorine atom ($I_{\text{Cl}} = 3/2$) and the aluminum atom ($I_{\text{Al}} = 5/2$) adds complex cascaded hyperfine splittings to each state. Though, the hyperfine splitting of the $X^1\Sigma^+$ state is smaller than the natural linewidth and remains unresolved.

Fig. 1 shows the corresponding detailed level scheme relevant to optical cycling in AlCl. The quantum num-

bers of the states are defined in Section II B. All Q-type transitions ($\Delta J = 0$) can be used for laser cooling since they are rotationally closed due to dipole and parity selection rules.

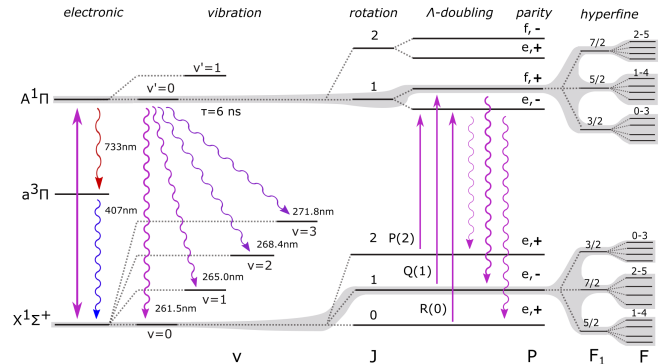


FIG. 1. Electronic and rovibrational energy level structure of AlCl. The Q transitions, which are used for laser cooling, are rotationally closed, unlike the P and R transitions. The manifolds of the $X^1\Sigma^+$ and $A^1\Pi$ states include 72 and 144 levels, respectively, all of which are involved in laser cooling AlCl. Adapted from [170].

A. Spectroscopy on AlCl

For the analysis in this work, two sets of data were used from two separate experiments, one in the Hemmerling group at the University of California, Riverside (UCR), and the other in the McCarron group at the University of Connecticut (UConn).

In the UCR group, AlCl is produced in a cryogenic helium buffer-gas beam source (CBGB) [171, 172] at 3.4 K via short-pulsed (5 ns) laser ablation of a Al:KCl mixture target [173] with a Nd:YAG laser (Mini-Lite II, Continuum) of ≈ 10 mJ per shot. More details on the source are described in Ref. [106]. The fluorescence data presented here was acquired ≈ 40 cm downstream from the source. The molecules were excited with laser light aligned orthogonal to the molecular beam direction and the induced fluorescence was collected with a photomultiplier tube (H10722-04, Hamamatsu). The excitation laser light of a few mW at 261.5 nm was produced by frequency-doubling the output of a 522 nm (VALO Vessel, Vexlum) with a custom-built second-harmonic generation cavity. The laser frequency was scanned and stabilized by using the frequency readout of a wavelength meter (WS-7, High-Finesse).

At UConn, the experimental approach is similar, with pulses of cold AlCl produced from a cryogenic buffer-gas beam source at 2.7 K via laser ablation (≈ 20 mJ at 532 nm). The source has been described previously in Ref. [174]. Molecules are optically addressed 94 cm downstream of the source below an EMCCD camera using ≈ 100 μW of laser light at 261.5 nm. This light is picked-off from a homebuilt laser system that generates

> 1 W in the fourth-harmonic from an infra-red fiber amplifier seeded by an external cavity diode laser (ECDL) at 1046 nm [114]. The EDCL is frequency stabilized and scanned using a transfer cavity locked to a frequency stabilized HeNe laser.

B. Hamiltonian of AlCl

In this section, the hyperfine energy level structure of the X - and A -electronic states are described in detail and the new molecular constants, which were acquired by using data from the spectroscopy setups, are discussed. Similar to the approach taken for AlF [82], we choose to describe both the $X^1\Sigma^+$ and $A^1\Pi$ states using a common Hund's case (a) coupling scheme. To describe the electronic state of AlCl, the total spin $\mathbf{J} = \mathbf{\Omega} + \mathbf{R}$, where \mathbf{R} is the rotational angular momentum and $\mathbf{\Omega} = \mathbf{\Lambda} + \mathbf{\Sigma}$ is the sum of the projection of the electron orbital angular momentum \mathbf{L} and the electron spin angular momentum \mathbf{S} on the internuclear axis. For the $X^1\Sigma^+$ state, the projections are $\Lambda = 0$ and $\Sigma = 0$. For the $A^1\Pi$ state, $\Lambda = \pm 1$ and $\Sigma = 0$. The hyperfine structure is accounted for by coupling \mathbf{J} to the nuclear spin of the aluminum atom, $\mathbf{F}_1 = \mathbf{J} + \mathbf{I}_{\text{Al}}$, which is in turn coupled to the nuclear spin of the chlorine atom, $\mathbf{F} = \mathbf{F}_1 + \mathbf{I}_{\text{Cl}}$.

a. X -State The Hamiltonian for the $X^1\Sigma^+$ state has the form [175]

$$H_X = H_0^X + H_{\text{EQ}} \quad , \quad (1)$$

where H_0^X includes the electronic, vibrational, and rotational energy terms, and H_{EQ} is the electric quadrupole term. H_0^X is expressed in terms of the Dunham expansion for $E(\nu, J)$ with equilibrium constants that have previously been measured [137].

The electric quadrupole interaction has previously been found to be the dominant hyperfine interaction in the $X^1\Sigma^+$ state [128], given as

$$H_{\text{EQ}} = \sum_{\alpha} \frac{\sqrt{6}(eQq_0)_{\alpha}}{4I_{\alpha}(2I_{\alpha} - 1)} T_0^2(\mathbf{I}_{\alpha}, \mathbf{I}_{\alpha}) \quad , \quad (2)$$

where α indicates the nucleus of aluminum and chlorine.

Constant	Value (MHz)
$(eQq_0)_{\text{Al}}$	-29.8(50)
$(eQq_0)_{\text{Cl}}$	-8.6(10)

TABLE I. Experimental electric quadrupole constants eQq_0 for the $X^1\Sigma^+$ state as measured in previous work [128].

Higher order terms, such as the nuclear-spin-rotation and the nuclear-spin-nuclear-spin interaction term are neglected, given the broad linewidth of the $A^1\Pi \leftarrow X^1\Sigma^+$ transition that is used in this study and the fact that these terms are expected to be two orders of magnitude smaller than the quadrupole terms, comparable to the case for the similar molecule AlF [82].

b. A -State For the $A^1\Pi$ state, the orbital angular momentum is non-zero. The orbital degeneracy of $\Lambda = \pm 1$ is lifted due to the presence of the end-over-end rotation of the molecule and results in a splitting of the rotational states into two opposite parity states, also known as Λ -doubling, see Fig. 1. The Hamiltonian for the $A^1\Pi$ state has the form [175]

$$H_A = H_0^A + H_{\text{LI}} + H_{\Lambda} + H_{\text{EQ}} + H_Z \quad (3)$$

where H_0^A includes the electronic, vibrational and rotational energy terms, H_{LI} is the nuclear-spin-orbital hyperfine term, H_{Λ} is the lambda-doubling term, H_{EQ} is the electric quadrupole term, and H_Z is the Zeeman term. H_0^A is expressed in the form of the Dunham expansion with equilibrium constants that have been measured in a previous study [106].

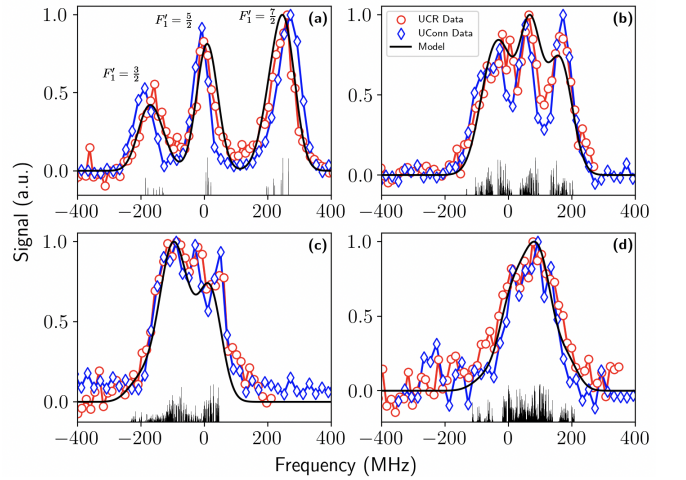


FIG. 2. Normalized fluorescence data (red circles: UCR, blue diamonds: UConn) and model (black solid line) of (a) R(0), (b) R(1), (c) R(2), and (d) R(3) of AlCl. The vertical black lines represent the different transitions predicted by our Hamiltonian model with their heights corresponding to their relative line strengths.

Due to the singlet nature of the $A^1\Pi$ state, the Λ -doubling term can be expressed as

$$H_{\Lambda} = - \sum_{k=\pm 1} e^{-2ik\phi} q T_{2k}^2(\mathbf{J}, \mathbf{J}) \quad (4)$$

and the nuclear-spin-orbital hyperfine term can be expressed as

$$H_{\text{LI}} = \sum_{\alpha} a_{\alpha} T^1(\mathbf{L}) \cdot T^1(\mathbf{I}_{\alpha}) \quad . \quad (5)$$

The quadrupole term for the $A^1\Pi$ state has both a component along and a component perpendicular to the internuclear axis

$$H_{\text{EQ}} = \sum_{\alpha} \frac{eQ_{\alpha}}{4I_{\alpha}(2I_{\alpha} - 1)} \left[\sqrt{6}q_{0,\alpha} T_0^2(\mathbf{I}_{\alpha}, \mathbf{I}_{\alpha}) + \sum_{k=\pm 1} e^{(-2ik\phi)} q_{2,\alpha} T_{2k}^2(\mathbf{I}_{\alpha}, \mathbf{I}_{\alpha}) \right] \quad . \quad (6)$$

The electric quadrupole constants are defined in terms of nuclear quadrupole moment, eQ , and electric-field-gradient at each nucleus, with q_0 being equal to the V_{zz} component and q_2 being equal to $2\sqrt{6}(V_{xx} - V_{yy})$ [175]. Based on our previous *ab initio* calculations [106], we performed additional *ab initio* calculations of the electric field gradients to get a theoretical estimate of the quadrupole constants, as shown in Tab. II and Tab. III. Using the quadrupole moments of 147.7 mb for the Al nucleus [147] and 85 mb for the ^{35}Cl nucleus [176], we find reasonable agreement between the theoretical and experimental values for the $X^1\Sigma^+$ state shown in Tab. I. This result increases our confidence in our *ab initio* values for the $A^1\Pi$ state.

Nucleus	State	V_{zz} (a.u.)	eQq_0 (MHz)
Al	$X^1\Sigma^+$	-0.809	-28.1
	$A^1\Pi$	-0.220	-7.6
Cl	$X^1\Sigma^+$	-0.675	-13.5
	$A^1\Pi$	-2.554	-51.0

TABLE II. *Ab initio* calculations of the electric field gradients and the quadrupole constants eQq_0 .

Nucleus	$2\sqrt{6}(V_{xx} - V_{yy})$ (a.u.)	eQq_2 (MHz)
Al	0.605	102.9
Cl	0.332	32.5

TABLE III. *Ab initio* calculations of the electric field gradients and the quadrupole constants eQq_2 for the $A^1\Pi$ state.

Given the broad linewidth of the $A^1\Pi \leftarrow X^1\Sigma^+$ transition, we use the following procedure to estimate the new equilibrium constants for the $A^1\Pi$ state. Starting with the R(0)-transition, we first use a least-squares fit to extract the hyperfine constants, a_{Al} and a_{Cl} , since the structure of this line is dominated by these parameters and much less affected by others. Then, with the hyperfine parameters set to their optimum values, we use a least-square fit to determine an upper limit of the Λ -doubling constant q by fitting the R(0)-R(3) transitions simultaneously. During the whole procedure, we keep the quadrupole constants, eQq_0 and eQq_2 , for both nuclei set to the values determined by the *ab initio* calculations.

Constant	Value (MHz)
a_{Al}	$131.9 \left(\begin{smallmatrix} +3.6 \\ -3.3 \end{smallmatrix} \right)$
a_{Cl}	$42.0 \left(\begin{smallmatrix} +8.1 \\ -7.0 \end{smallmatrix} \right)$
q	< -3.0

TABLE IV. Molecular constants for the $A^1\Pi$ state obtained in this work.

The resulting equilibrium constants are presented in Tab. IV. The errors of the constants correspond to a $\approx 2.5\%$ deviation of the absolute value of the residuals of the fit and model from the optimal value. We note that the value for the Λ -doubling constant is an upper limit since it is mainly determined by the width of the

broad features of R(2) and R(3). Our approach yields a good agreement between both independent data sets, UCR and UConn, and the Hamiltonian model using the combination of fitted and *ab initio* values for the molecular constants, as shown in Fig. 2. We note that a small discrepancy between the two data sets shown in Fig. 2 (a). We attribute this to the nonlinearity of the transfer cavity used in the UConn laser frequency stabilization scheme. Here, the frequency of the ECDL inherits the nonlinearity of the transfer cavity, which is exacerbated by the o-rings used in its design [177]. This nonlinearity depends on the cavity DC value and was not a significant effect in the other R-line scans. For this reason, only the UCR data were used to fit the R(0) transition. This highlights that, while transfer cavities are effective for frequency stabilization, care must be taken when using this approach for spectroscopy, especially where subsequent stages of second- or fourth-harmonic generation amplify these non-linearities.

Finally, overlaying the model with the parameters acquired through the R-transitions with the fluorescence measurements of the Q-branch at UCR and UConn yields a reasonable agreement, as shown in Fig. 3. We note that the Q-branch fit has no free parameters besides the overall frequency offset, the rotational temperature (2.5 K/1.6 K for the UCR/UConn data) and the overall amplitude. Finally, the density of the lines of the Q-transitions illustrates the similarity of the rotational constants of the $X^1\Sigma^+$ and $A^1\Pi$ states, which in part leads to the predicted highly diagonal Franck-Condon factors of AlCl [106].

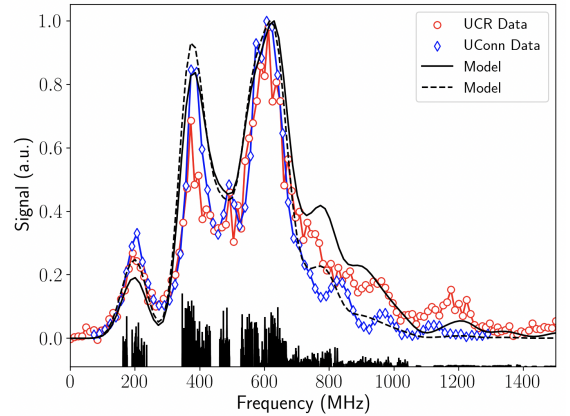


FIG. 3. Normalized fluorescence data (red circles: UCR data, blue diamonds: UConn data) and model (black solid line) of the Q(0)-Q(5) transitions of AlCl. The models use the fitting parameters of the R-lines from Tab. IV and only optimizes for the overall signal amplitude, the rotational temperature ($T_{\text{rot}} = 2.5$ K solid line, $T_{\text{rot}} = 1.6$ K dashed line) and the absolute frequency offset. The vertical black lines represent the different transitions predicted by our Hamiltonian model with their heights corresponding to their relative line strengths.

C. Zeeman Splitting

To set up a magneto-optical trap for a new species, it is important to fully understand the Zeeman splitting of the cooling transition in order to design the magnetic field gradients appropriately. In the case of AlCl, the dominant Zeeman term in the $A^1\Pi$ state is the interaction between the electron-orbital-angular-momentum, \mathbf{L} , and the applied magnetic field, \mathbf{B} . This interaction has the form

$$H_Z = g_L \mu_B T^1(\mathbf{L}) \cdot T^1(\mathbf{B}) \quad (7)$$

where $g_L = 1$ and μ_B is the Bohr magneton. The dominant Zeeman interaction in the $X^1\Sigma^+$ state is the nuclear-spin-Zeeman interaction, $\mathbf{I}_\alpha \cdot \mathbf{B}$, which has a magnetic dipole moment that is smaller than the $A^1\Pi$ state by a factor of m_e/m_p , where m_e is the electron mass and m_p is the proton mass. Thus, the Zeeman splitting of the $X^1\Sigma^+$ state is negligible and Zeeman shifts on the cycling transition are fully determined by the splitting of the $A^1\Pi$. We show the calculated Zeeman splitting of the $A^1\Pi$, ($v' = 0, J' = 1$) state as a function of an external magnetic field in Fig. 4. This is our principle target excited state for optical cycling in AlCl using the $Q(1)$ cycling transition. However, the close proximity of other Q -transitions means that a single laser frequency will likely address and lead to optical cycling for molecules in multiple low-lying rotational states within the electronic ground state, see Fig. 3.

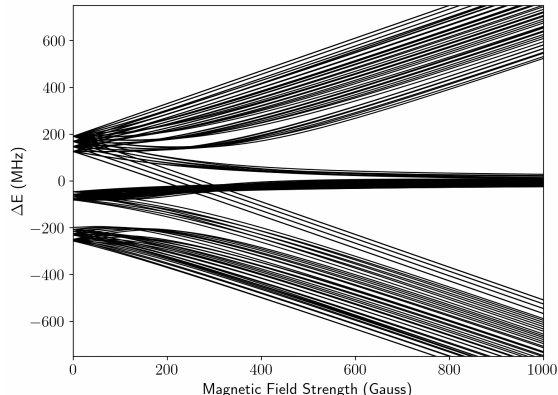


FIG. 4. The Zeeman splitting of the $A^1\Pi$, ($v' = 0, J' = 1$) manifold of AlCl as a function of the external magnetic field is shown.

In the low field regime, magnetic sublevels are shifted linearly according to Landé g -factors that vary in both magnitude and sign for different hyperfine states, see table Tab. V for the g -factors of the target even parity $A^1\Pi$, ($v' = 0, J' = 1$) excited state. While in principle this structure can lead to magnetically tunable transitions for use in a Zeeman slower, the large hyperfine spread of the J' states within the $A^1\Pi$ state combined with the lack of a type-I transition, can make addressing individual velocity classes challenging.

Realizing confining transitions in a MOT of AlCl to the $F_1 = 5/2$ and $7/2$ manifolds will require an orthogonal circular laser polarization compared to confining transitions to the $F_1 = 3/2$ manifold since these states have g -factors with opposite sign. We emphasize that a MOT of AlCl appears similar in nature to atomic type-II MOTs. Here the magnetically tunable states that enable confinement are in the electronic excited state and decay rapidly via spontaneous emission to the unresolved and unperturbed $X^1\Sigma^+$ ground state. By contrast, in $^2\Sigma$ -type molecules, the dominant Zeeman shift is in the ground state, which can lead to stationary magnetic dark states that require either static dual-frequencies [178] or rapid synchronous switching of the field gradient and laser polarizations [179, 180] to generate substantial confining forces. While the general level structure and Zeeman shifts within molecules with $^1\Sigma$ ground states may simplify magneto-optical trapping methods, coherent dark states may still need to be addressed, see Section III D and Ref. [181].

In Tab. V, we list the Landé factors for low magnetic fields (< 10 Gauss) of the different hyperfine states in the even parity $A^1\Pi$, ($v' = 0, J' = 1$) manifold. We note that a MOT of AlCl will require a large magnetic field gradient on the order of 100 G/cm axially to realize confining forces due to the small excited state g -factors and the large transition linewidth. This is similar to MOTs using strong transitions in alkaline earth and alkaline earth-like atoms [182].

F_1	F	g_F	F_1	F	g_F	F_1	F	g_F
3/2			5/2			7/2		
	0	-		1	0.15			
	1	-0.15		2	0.07		2	0.23
	2	-0.13		3	0.05		3	0.15
	3	-0.12		4	0.03		4	0.12
							5	0.10

TABLE V. Calculated Landé factors of the even parity $A^1\Pi$ ($v = 0, J' = 1$) states of AlCl.

Finally, in the high-field regime, the different spins decouple and the overall state structure simplifies into three manifolds, each of which has common Landé factors. This Paschen-Back regime has been proposed for a Zeeman slowing scheme for CaF at ≈ 300 Gauss [183]. Though, AlCl would require even higher fields and field-gradients to completely isolate the manifolds, we note that MOTs with gradients of ≈ 1 kGauss/cm have been realized [184–186].

III. OPTICAL CYCLING

The strong optical cycling $A^1\Pi - X^1\Sigma^+$ ($v = 0, v' = 0$) transition near 261.5 nm combines a large linewidth ($2\pi \times 25$ MHz) with a large photon recoil velocity (2.5 cm/s) to offer access to strong radiative forces.

These forces could potentially slow a molecular beam from a cryogenic source to below the capture velocity of a MOT in just a few centimeters, rather than the ≈ 1 m required for today's experiments with $^2\Sigma$ molecules [93, 97, 99, 100, 102]. Such an improvement would increase the solid-angle and trappable flux from a cryogenic source by several orders-of-magnitude and tackle inefficient MOT loading, which remains a key bottleneck in the field of molecular laser cooling and trapping. Alternatively, new slowing techniques, such as bichromatic slowing [187–192], travelling-wave Stark deceleration [193–199] or Zeeman-Sisyphus deceleration [91], may offer solutions to this challenge. Strong, short-wavelength optical transitions, such as those in AlCl, AlF and MgF, are attractive for laser cooling and trapping but demand high laser intensity since the saturation intensity scales as $I_{\text{sat}} \propto \Gamma/\lambda^3$. The AlCl optical cycling transition at 261.5 nm is particularly fortuitous since ytterbium fiber lasers and amplifiers offer high power (10–100 W) at the fundamental of the forth-harmonic (1046 nm) and 261.5 nm is close enough to the frequency quadrupled Nd:YAG that optics are well-developed and commercially available. In the following, we outline the prospects of optical cycling in the different ro-vibrational and hyperfine manifolds of AlCl and compare the effects to other molecules, AlF and TlF.

A. Vibrational branching

AlCl is expected to have highly diagonal Franck-Condon factors (FCFs) which limit decay into excited vibrational levels within the $X^1\Sigma^+$ manifold during optical cycling. Previous work by multiple groups predict a FCF in the $v'' = 0$ band of $q_{00} > 0.99$ [56, 105, 106, 149] with ~ 3 lasers (one cycling laser and two repumps) being sufficient to scatter the $\sim 10^4$ photons required to slow, laser cool and trap [90, 93]. Experimental work to directly confirm this diagonal vibrational branching is underway [200], similar to previous work with TlF [201], BH [202] and AlF [82], other candidate molecules for laser cooling experiments with $^1\Sigma$ ground states. We note in passing that the single unpaired valence electron within each $^2\Sigma$ molecule laser cooled to-date offers an intuitive picture behind the origin of diagonal FCFs, i.e. that the optically-addressable electron plays a negligible role in the binding of the molecule. By contrast, to the best of our knowledge, no similar intuition can be used to identify closed-shell $^1\Sigma$ molecules with diagonal FCFs.

B. Rotational branching

Rotational branching within AlCl can be tamed using selection rules that dictate the allowed changes in angular momentum and wavefunction symmetry (parity) during electronic transitions [68]. Namely, the electric dipole transitions with nonzero transition dipole matrix

elements (TDME) are limited to $\Delta J = 0, \pm 1$ and, because the dipole operator is a rank 1 tensor (odd), the wavefunctions of the connected states must have opposite parity. For $^1\Sigma$ ground state molecules, such as AlCl, these selection rules enable rotational closure for all Q-transitions ($\Delta J = 0$) (see Fig. 1).

A loss channel via rotational branching can be introduced by a small electric field to mix the closely spaced opposite parity Λ -doublets in the $A^1\Pi$ state and hence break the parity selection rule. In this case for AlCl, spontaneous emission would then populate dark rotational states via the P- and R-branches ($\Delta J = -1$ and $+1$, respectively). This loss mechanism was reported in a radio-frequency MOT of SrF molecules [180] and, notably, has been investigated for AlF [203], with this loss channel becoming negligible for stray fields below 1 V/cm. For AlCl, the level of electric field suppression required remains unclear as our spectra can only place an upper bound on the Λ -doubling parameter q that dictates the spacing between Λ -doublets, see Tab. IV.

An additional loss mechanism, enabling transitions with $|\Delta J| > 1$, can result from mixing between states with the same total angular momentum F from different rotational levels within the excited electronic state. In both AlCl and AlF, this mixing in the $A^1\Pi$ state is predominantly due to the magnetic hyperfine interaction of the Al nuclear spin and is expected to result in a small loss channel of order 10^{-6} [82, 170]. By contrast, this mixing and rotational branching in TlF can be substantial and poses a challenge to optical cycling in this molecule [67].

C. Hyperfine Structure

The Al and Cl nuclear spins result in AlCl having a complex hyperfine structure, with 12 hyperfine states for $J = 1$, 18 for $J = 2$, 22 for $J = 3$ and 24 for $J \geq 4$, respectively (see Fig. 1). In the $X^1\Sigma^+$ state, the lack of spin-orbit coupling results in the hyperfine structure being small and unresolved to the strong $A^1\Pi - X^1\Sigma^+$ transition ($\Gamma \approx 2\pi \times 25$ MHz). For example, in $J = 1$ all 12 hyperfine states span just ≈ 11 MHz [128]. While this allows all ground state hyperfine levels for a given J to be conveniently addressed by a single laser frequency, it can also lead to the formation of slowly evolving dark states which prevent rapid optical cycling (see Section III D).

In the $A^1\Pi$ state, the hyperfine structure is at best only partially resolved for low-lying rotational states (see Fig. 2). Our analysis shows that, similar to AlF [82], this structure is primarily due to the nuclear spin-electron orbit interaction with the eQq_0 and eQq_2 constants dictating that the electric quadrupole interaction only plays a small role. Interestingly, the $A^1\Pi$ ($v' = 0, J' = 1$) hyperfine structure spans ~ 500 MHz, equivalent to a Doppler spread of ~ 130 m/s at 261.5 nm. This, combined with power broadening, may enable a single laser frequency to address the decreasing Doppler shift of molecules during

laser slowing without the need for frequency chirping or phase modulating the slowing light.

For convenience, we use a Hund's case (a) basis to describe the AlCl ground and excited states using quantum numbers F and F_1 (see above). However, we emphasize that F_1 is not a good quantum number and states with common F from different F_1 are mixed. In AlCl, this mixing arises in the $X^1\Sigma^+$ state due to the quadrupole interaction with the Cl nuclear spin and in the $A^1\Pi$ state due to the Cl nuclear spin-electron orbit interaction. While this mixing does not lead to loss from the optical cycle, it does skew hyperfine branching ratios away from the unmixed case [170].

D. Dark States

Rotational structure in molecules dictates that optical cycling requires type-II transitions which naturally introduce dark states within the ground electronic state [44, 204]. In general, these can be either stationary angular momentum eigenstates, in which molecules accumulate and leave the optical cycle, or a coherent superposition of these eigenstates, which naturally precess between bright and dark states, limiting the maximum photon scattering rate [205, 206].

For $^2\Sigma$ molecules, it is common to remix dark states using a Zeeman shift to lift the degeneracy of ground state sublevels by $\sim \Gamma$. This approach is impractical for $^1\Sigma$ molecules due to their small ground state magnetic moments which, coupled with their unresolved ground state hyperfine splittings, can result in robust, slowly-evolving coherent dark states which significantly limit photon scattering rates. Fortunately, rapid polarization switching offers an alternative method to address stationary dark states and also destabilize coherent dark states, provided that the number of ground states is less than three times the number of available excited states, i.e. a single laser polarization addresses more than $\frac{1}{3}$ of ground states. While this can be the case for Q-transitions in AlCl and AlF [82], it is not the case for TIF [103, 104, 180] where the excited state hyperfine structure is well resolved. In this case, additional switched microwave fields linking rotational states in the electronic ground state are required.

The dark state composition in AlCl was calculated following the method in Refs. [46, 204], with the number of dark states for the $Q(1)$ transition depending on the number of partially resolved excited states addressed. Assuming power broadening is adequate to address the entire $A^1\Sigma(v' = 0, J' = 1)$ state, we find that, in the absence of a magnetic field, π -transitions driven by linearly polarized light lead to 24 coherent dark states and no stationary dark states, indicating no leakage from the optical cycle but a constraint on the maximum photon scattering rate for a fixed laser polarization.

A similar calculation for the dark state composition in AlF is described in Ref. [203]. Here dark states are

formed by linear superpositions of states with different values of F_1 and the limit on the scattering rate is consistent with the smallest splitting among them. In AlCl, the dark state composition is more complicated, with dark states described instead by superpositions between states with different F_1 , F , and m_F quantum numbers, leading to dark states between both magnetic and hyperfine levels. Ongoing experimental work will test these results by measuring photon scattering rates in AlCl with and without polarization modulation [200].

IV. ESTIMATE OF THE CAPTURE VELOCITY OF A MAGNETO-OPTICAL TRAP FOR ALCL

To load AlCl into a magneto-optical trap, molecules need to be slowed to (or below) the MOT capture velocity. This step is necessary for molecular MOTs since, in contrast to their atomic counterparts, the beam sources that are bright enough for a realistic experiments typically are not effusive in nature. Instead, the molecular sources, e.g. a cryogenic buffer gas beam or a super-sonic beam, have a boosted forward velocity distribution with higher average values and widths that are too narrow to provide a sufficient flux of molecules below the MOT's capture velocity. Hence, currently a slowing stage is essential before molecules can be trapped in a MOT. In current MOT experiments, both white-light [207, 208] and chirped slowing [100, 209] are successfully used to prepare beams for trapping. Since the momentum imparted by each photon recoil is small, it is necessary to cycle many photons ($\gtrsim 10^4$), see Section III. We note that alternative slowing methods that avoid the need for repeated photon scattering, are being explored in the community. Examples include the bichromatic force [187–192], travelling-wave Stark deceleration [193, 194] and Zeeman-Sisyphus deceleration [91].

To estimate the MOT capture velocity, and threshold that needs to be reached by the slowing process, we numerically simulate the dynamics of AlCl molecules entering a MOT. Here, we use a standard 3D-MOT configuration comprised of a quadrupole magnetic field gradient of 75 G/cm axially and three pairs of retro-reflected laser beams, each with a Gaussian beam profile. We then implement the Hamiltonian from Section II and the MOT configuration in the open source Python package PyLCP [210] and solve for the time evolution of the trajectories of AlCl.

The presence of both hyperfine spins in AlCl leads to a large number of quantum states in each rotational manifold that must be included to fully describe the system. In general, capturing the effects of coherences in simulations requires evaluating the optical Bloch equations [181, 211, 212]. However, the optical cycling transition $X^1\Sigma^+ |v = 0, J = 1\rangle \leftrightarrow A^1\Pi |v' = 0, J' = 1\rangle$ involves 144 magnetic sublevels rendering a full simulation computationally challenging. As a result, we perform the following estimates of the capture velocity using rate

equations and therefore expect this approach to break down as laser intensity grows and coherent dark states begin to limit excitation. By trading intensity for MOT beam diameter, we will operate near the saturation intensity ($\approx 232 \text{ mW/cm}^2$ for AlCl), where other molecules have been shown to be well described by rate equations [178, 203].

We simulate the molecular trajectories for different initial velocities and laser powers and extract the maximum molecular velocity that is captured for a range of MOT beam diameters. The cooling lasers that address the $X^1\Sigma^+ |v=0, J=1\rangle \leftrightarrow A^1\Pi |v'=0, J'=1\rangle$ transition are detuned by $-\frac{\Gamma}{2}$ from the $F'_1 = 7/2$ level. We further assume that no vibrational branching occurs during the simulation, i.e. the repump lasers have been applied accordingly. We also reduce the calculated equilibrium force by a factor of two at each timestep of the simulation to account for the Λ -system created between the cycling and the first repump lasers [213].

The results of these simulations are shown in Fig. 5. We find that a MOT capture velocity $v_{\text{cap}} \geq 30 \text{ m/s}$ requires a mean intensity in the range $\sim 0.1 - 1 \text{ W/cm}^2$ per beam, depending on the MOT beam diameter (d), with smaller beams requiring higher intensity (and higher scattering rates, R_{sc}) to account for shorter interaction times. These results follow the general results of a simplified two-level model, as discussed in Ref. [170]. In brief, for a fixed beam diameter d , $v_{\text{cap}} \propto \sqrt{d \cdot R_{\text{sc}}}$. At low intensity I , for fixed laser power, $R_{\text{sc}} \propto I \propto d^{-2}$ and so $v_{\text{cap}} \propto d^{-1/2}$. At higher intensity towards saturation, this dependence is weakened since now $R_{\text{sc}} \propto d^{-m}$ where $0 \leq m < 2$, with $m = 0$ representing when the transition is fully saturated, and so $v_{\text{cap}} \propto d^{(1-m)/2}$.

While a large MOT capture velocity is desirable, it is also important to consider the spatial overlap between the MOT volume and the slowed molecular beam, which has a solid angle $\Omega_s \propto d^2$. In general, the number of trapped molecules $N_{\text{MOT}} \propto \Omega_s \cdot v_{\text{cap}}^\kappa$ where κ is determined by the slowed beam's velocity profile. Typically, $\kappa > 1$ since there can be many more molecules available for capture at higher velocities due to reduced transverse beam divergence [207] and this gives rise to two regimes. When below saturation, due to limited laser power, as could be the case in the deep UV for AlF, smaller MOT beams are desirable since here $N_{\text{MOT}} \propto d^{2-\kappa/2}$ with $(2 - \kappa/2) < 0$. By contrast, when transitions can be saturated using high laser power, $N_{\text{MOT}} \propto d^{2+\kappa(1-m)/2}$ with $2 + \kappa(1-m)/2 > 0$, and large MOT beams are optimal. This high power, large diameter regime is typically where today's molecular MOTs using $^2\Sigma$ molecules operate when loading. Our goal is to also operate towards this regime for AlCl using $\sim 1 \text{ cm } 1/e^2$ diameter beams each with $\sim 0.5 \text{ W}$. However, our ongoing work probing the scattering rate vs intensity [200] will ultimately guide our MOT beam parameters to use the available laser power [174] most efficiently to maximize N_{MOT} .

While high intensity and large scattering rates are beneficial for MOT loading, it is common to reduce the inten-

sity immediately after loading. This reduces the scattering rate which both cools the trapped atoms by limiting Doppler heating and increases the trap lifetime for state preparation or transfer to a conservative trap. This step will also likely be important for an AlCl MOT since the Doppler temperature is $600 \mu\text{K}$. A blue-detuned MOT of AlCl, as recently demonstrated for YO [214] and SrF [48], could potentially cool below this limit towards the recoil temperature of $5 \mu\text{K}$, though substantial vibrational closure would be needed for efficient transfer from the red-detuned MOT since these blue-detuned MOTs operate at high intensity and require $> 20 \text{ ms}$ to load [48].

For short wavelength transitions at high intensity, one also needs to consider the possibility of significant loss via photo-dissociation and photo-ionization of the molecule. The latter effect has been known to dominate loss processes in atomic MOTs [215]. Here, we carry out *ab initio* calculations on the cross-sections of AlCl for these processes to characterize their effect.

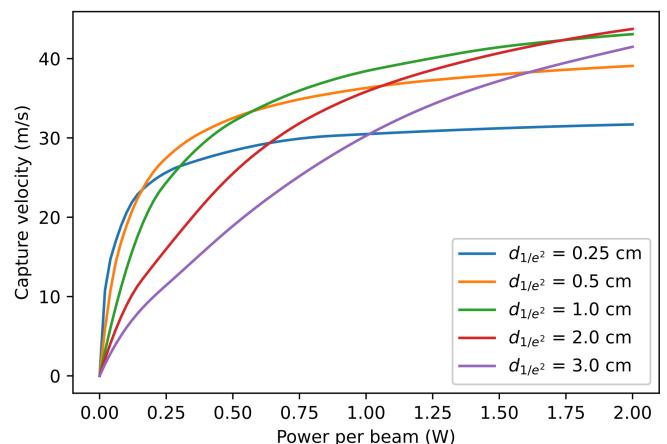


FIG. 5. Simulated capture velocities plotted as a function of laser power per beam for different beam diameters. The beam diameter is defined as the $1/e^2$ diameter of the Gaussian beams. Figure reproduced from Ref. [170].

V. PHOTO-DISSOCIATION AND IONIZATION OF ALCL

In this section, we analyze the two-photon process that can lead to photo-induced dissociation and ionization. Fig. 6 plots selected potential energy curves (PECs) for AlCl. The lowest three black curves are based on *ab initio* calculations that have been fit to Morse potentials [106]. These PECs correlate asymptotically for large internuclear separation (r) to the dissociation energy of neutral Al + Cl. The two relevant excited electronic state PECs are plotted in blue and red for the $2^1\Pi$ and $3^1\Sigma^+$ states, respectively. Asymptotically for large r the $2^1\Pi$ PEC approaches the dissociation energy of neutral Al + Cl whereas the $3^1\Sigma^+$ PEC approaches the dissociation en-

ergy of ionic $\text{Al}^+ + \text{Cl}^-$. These PECs are based on fitting repulsive exponential functions ($V = V_o \exp[\alpha(r - r_o)^2]$) to the *ab initio* data reported in Ref. [109]. The V_o , α , and r_o are adjustable fitting parameters and were optimized to minimize the root-mean-square error between the analytic curves and the *ab initio* data.

A simplex fitting algorithm was used (AMOEBA [216]) and the optimal parameters were determined to be $V_o = 4.40249 \times 10^4 \text{ cm}^{-1}$, $\alpha = 0.174950 \text{ \AA}^{-2}$, and $r_o = 3.73886 \text{ \AA}$ for the $2^1\Pi$ state and $V_o = 4.53576 \times 10^4 \text{ cm}^{-1}$, $\alpha = 6.76293 \times 10^{-2} \text{ \AA}^{-2}$, and $r_o = 4.89511 \text{ \AA}$ for the $3^1\Sigma^+$ state (the fitted parameters quoted above include several extra digits for numerical reasons to ensure that the potential curves can be accurately reproduced). The vertical black and red dashed arrows represent the two-photon excitation process that can lead to dissociation along the repulsive $2^1\Pi$ PEC (blue) or ionization along the repulsive $3^1\Sigma^+$ PEC (red). From these PECs we can compute intensity profiles for the dissociation and ionization cross sections by calculating the Franck-Condon overlaps between the ground ro-vibrational eigenfunction of the $A^1\Pi$ state with the continuum eigenstates of the $2^1\Pi$ and $3^1\Sigma^+$ states, respectively.

The reflection technique is used where the continuum eigenfunctions are represented by delta functions located at the classical turning points along the repulsive PECs [217]. The intensity profiles are then simply proportional to $\nu \psi_0^2$ where ν is the excitation energy and ψ_0 is the ground ro-vibrational wave function evaluated at the r corresponding the classical turning point for the energy ν . We can derive the classical turning points r_c as a function of ν from the exponential functions given above by setting $V = \nu$ to obtain $r_c = r_o - \sqrt{\ln(\nu/V_o)}/\alpha$.

An energy grid in ν was constructed using 100 points between 6.0 and $8.5 \text{ cm}^{-1} (\times 10^4)$. The ground ro-vibrational wavefunction for the $A^1\Pi$ state (computed in our previous work [106]) was then evaluated at each of the corresponding r_c values and the resulting intensity profiles (normalized) are plotted in Fig. 7 for both dissociation (solid blue) and ionization (solid red). For reference, the energies of the two relevant laser wavelengths (265 and 261 nm) are plotted with black vertical lines. From these profiles, it is clear that these laser wavelengths could lead to photo-ionization via the excited $3^1\Sigma^+$ state but dissociation via the $2^1\Pi$ state is unlikely. The sensitivity of the profiles plotted in Fig. 7 on the exponential fits was quantified by increasing and decreasing the slopes of the PECs by approximately 1.5% (the dashed and long-short dashed red and blue curves in Fig. 6). The corresponding cross sections are plotted with dashed and long-short dashed red and blue curves in Fig. 7.

VI. CONCLUSION

We have characterized the hyperfine structure of the $A^1\Pi$ state in AlCl and reported the first measurement

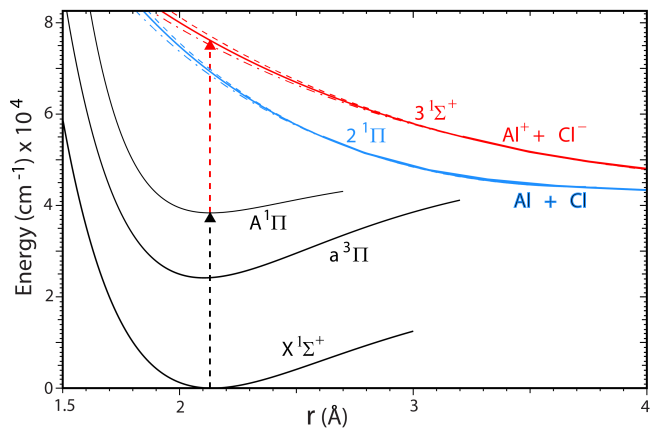


FIG. 6. Five selected potential energy curves (PECs) are plotted for AlCl as a function of the internuclear distance r . The three black and one blue PECs correlate to neutral Al + Cl dissociation for large r whereas the red PEC leads to ionization $\text{Al}^+ + \text{Cl}^-$. The two-photon process is indicated by the vertical dashed black and red arrows.

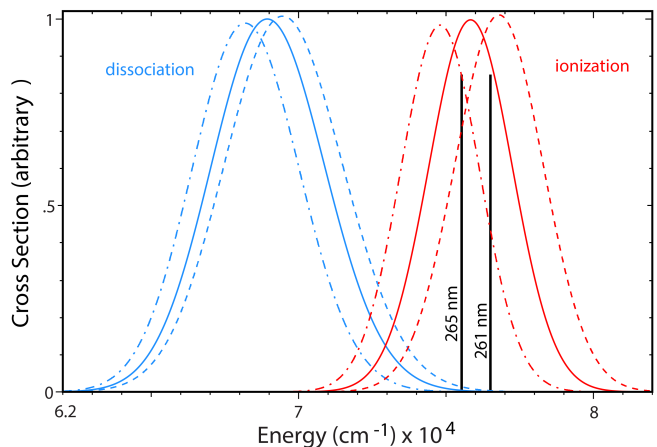


FIG. 7. The normalized photo-dissociation (blue) and photo-ionization (red) cross sections are plotted as a function of the excitation energy. The energies of the two relevant laser wavelengths (261 nm: main cooling transition, and 265 nm: 1st vibrational repumper) are indicated by the vertical black lines. The dashed and short-long dashed curves quantify the sensitivity of the cross sections to the slopes of the potential energy curves of the repulsive excited electronic states (see Fig. 6).

of the nuclear spin-electron orbit interaction strength of the excited state. We discuss strategies and possible loss mechanisms for efficient optical cycling and compare the advantages of AlCl to other molecules. Both AlCl and AlF have similar internal structures and are expected to allow for similar cooling schemes. While the larger linewidth and shorter wavelength of AlF results in access to larger optical forces, the AlF saturation intensity is $4\times$ higher than AlCl which poses significant demands on the laser technology and optics required. An additional advantage of AlCl (and AlF) is that transitions

can simultaneously be driven to multiple excited states, allowing polarization modulation to destabilize coherent dark states, in contrast to TIF. The larger ground state hyperfine splittings in AlCl and AlF also result in these dark states naturally precessing into bright states more rapidly than in the case of TIF.

Finally, the hyperfine structure in the $A^1\Pi$ state studied in this work spans between $\sim 250 - 500$ MHz for $J' = 1 - 4$ while the $X^1\Sigma^+$ hyperfine structure is unresolved for the cycling transition. While such a broad excited state spread makes addressing individual velocity classes challenging using a type-II transition in, for example, a Zeeman slower, it does potentially offer two advantages. First, increased scattering rates may be accessed by targeting different excited hyperfine states with the cycling and first repump lasers to avoid coupling these lasers and creating a Λ -system. This approach is similar to that used with alkali atoms. Second, laser slowing may be simplified since a single laser frequency can simultaneously address a broad range of velocities, similar to white light or frequency chirped slowing, but without the need to spectrally or temporally dilute the laser intensity applied to each velocity. This may allow a single laser frequency to slow molecules directly from a single-stage CBGB and reduce the technical complexity.

We use numerical simulation of the full AlCl Hamiltonian to estimate the capture velocity of a magneto-optical trap for AlCl. Our results yield capture velocities of up to $30 - 40$ m/s when using ≈ 1 W of laser power per MOT beam, suggesting that a significant part of a CBGB source with a slowing cell [218] could be directly loaded into a MOT without slowing. This result highlights another advantage of AlCl, but should also be understood in the context of MOT capture velocities of other molecules, where magnitudes for CaF of $5 - 20$ m/s [48, 101, 178, 219], for SrF of $9 - 13$ m/s [48], and for

MgF of 26 m/s [220] have been either calculated or measured. Optimization strategies for increasing these values to higher magnitudes have been explored as well [221].

Finally, a possible limit preventing a high-intensity MOT for AlCl is that two-photon excitation may lead to substantial trap loss. Using *ab initio* calculations of the excitation cross-sections, we identified that photo-ionization via a dissociative $2^1\Sigma^+$ state could be a non-negligible loss process when using the main cycling and the first vibrational repump transition for the MOT. To the best of our knowledge, as yet there are no available experimental data on this process, which is required to verify if photo-ionization will indeed limit the lifetime of an AlCl MOT.

ACKNOWLEDGMENTS

J.R.D., C.W., L.-R.L., and B.H. acknowledge funding from the NSF grant number 1839153 and from the AFRL grant number FA9550-21-1-0263. B.K.K. acknowledges that part of this work was done under the auspices of the U.S. Department of Energy under Project No. 20170221ER of the Laboratory Directed Research and Development Program at Los Alamos National Laboratory. Los Alamos National Laboratory is operated by Triad National Security, LLC, for the National Nuclear Security Administration of the U.S. Department of Energy (Contract No. 89233218CNA000001). J.C.S. and D.J.M. gratefully acknowledge funding from the NSF (grant number 1848435), and the University of Connecticut College of Liberal Arts and Sciences and the Office of the Vice President for Research.

-
- [1] V. Andreev, D. G. Ang, D. DeMille, J. M. Doyle, G. Gabrielse, J. Haefner, N. R. Hutzler, Z. Lasner, C. Meisenhelder, B. R. O'Leary, C. D. Panda, A. D. West, E. P. West, X. Wu, and ACME Collaboration, "Improved limit on the electric dipole moment of the electron," *Nature* **562**, 355–360 (2018).
 - [2] William B. Cairncross, Daniel N. Gresh, Matt Grau, Kevin C. Cossel, Tanya S. Roussy, Yiqi Ni, Yan Zhou, Jun Ye, and Eric A. Cornell, "Precision measurement of the electron's electric dipole moment using trapped molecular ions," *Phys. Rev. Lett.* **119**, 153001 (2017).
 - [3] Ivan Kozyryev and Nicholas R. Hutzler, "Precision measurement of time-reversal symmetry violation with laser-cooled polyatomic molecules," *Physical Review Letters* **119**, 133002 (2017).
 - [4] J J Hudson, D M Kara, I J Smallman, B E Sauer, M R Tarbutt, and E A Hinds, "Improved measurement of the shape of the electron," *Nature* **473**, 493–496 (2011).
 - [5] Ivan Kozyryev, Zack Lasner, and John M. Doyle, "Enhanced sensitivity to ultralight bosonic dark matter in the spectra of the linear radical sroh," *Physical Review A* **103**, 043313 (2021).
 - [6] S. S. Kondov, C.-H. Lee, K. H. Leung, C. Liedl, I. Majewska, R. Moszynski, and T. Zelevinsky, "Molecular lattice clock with long vibrational coherence," *Nature Physics* **15**, 1118–1122 (2019).
 - [7] The ACME ACME Collaboration, J Baron, W C Campbell, D DeMille, J M Doyle, G Gabrielse, Y V Gurevich, P W Hess, N R Hutzler, E Kirilov, I Kozyryev, B R O'Leary, C D Panda, M F Parsons, E S Petrik, B Spaun, A C Vutha, and A D West, "Order of magnitude smaller limit on the electric dipole moment of the electron," *Science* **343**, 269–72 (2014).
 - [8] N. J. Fitch, J. Lim, E. A. Hinds, B. E. Sauer, and M. R. Tarbutt, "Methods for measuring the electron edm using ultracold ybf molecules," *Quantum Sci. Technol.* **6**, 014006 (2021).
 - [9] Phelan Yu and Nicholas R. Hutzler, "Probing fundamental symmetries of deformed nuclei in symmetric top molecules," *Physical Review Letters* **126**, 023003 (2021).

- (2021).
- [10] Nicholas R. Hutzler, “Polyatomic molecules as quantum sensors for fundamental physics,” *Quantum Science and Technology* **5**, 44011 (2021).
 - [11] Matthew J. O’Rourke and Nicholas R. Hutzler, “Hypermolecular polar molecules for precision measurements,” *Physical Review A* **100**, 022502 (2019).
 - [12] Parul Aggarwal, Hendrick L. Bethlem, Anastasia Borschevsky, Malika Denis, Kevin Esajas, Pi A.B. Haase, Yongliang Hao, Steven Hoekstra, Klaus Jungmann, Thomas B. Meijknecht, Maarten C. Mooij, Rob G.E. Timmermans, Wim Ubachs, Lorenz Willmann, and Artem Zapara, “Measuring the electric dipole moment of the electron in baf,” *European Physical Journal D* **72**, 197 (2018).
 - [13] Jean-Philippe Uzan, “The fundamental constants and their variation: observational and theoretical status,” *Reviews of Modern Physics* **75**, 403 (2003).
 - [14] D. DeMille, S. Sainis, J. Sage, T. Bergeman, S. Kotochigova, and E. Tiesinga, “Enhanced sensitivity to variation of m_e/m_p in molecular spectra,” *Physical Review Letters* **100**, 043202 (2008).
 - [15] Cheng Chin, V V Flambaum, and M G Kozlov, “Ultracold molecules: new probes on the variation of fundamental constants,” *New Journal of Physics* **11**, 55048 (2009).
 - [16] Masatoshi Kajita, “Sensitive measurement of m_p/m_e variance using vibrational transition frequencies of cold molecules,” *New Journal of Physics* **11**, 055010 (2009).
 - [17] K. Beloy, A. Borschevsky, P. Schwerdtfeger, and V. V. Flambaum, “Enhanced sensitivity to the time variation of the fine-structure constant and j span class,” *Physical Review A* **82**, 022106 (2010).
 - [18] Paul Jansen, Hendrick L. Bethlem, and Wim Ubachs, “Perspective: Tipping the scales: Search for drifting constants from molecular spectra,” *The Journal of Chemical Physics* **140**, 010901 (2014).
 - [19] M. Daprà, M. L. Niu, E. J. Salumbides, M. T. Murphy, and W. Ubachs, “Constraint on a cosmological variation in the proton-to-electron mass ratio from electronic absorption,” *The Astrophysical Journal* **826**, 192 (2016).
 - [20] J. Kobayashi, A. Ogino, and S. Inouye, “Measurement of the variation of electron-to-proton mass ratio using ultracold molecules produced from laser-cooled atoms,” *Nature Communications* **10**, 1–5 (2019).
 - [21] T. E. Chupp, P. Fierlinger, M. J. Ramsey-Musolf, and J. T. Singh, “Electric dipole moments of atoms, molecules, nuclei, and particles,” *Reviews of Modern Physics* **91**, 015001 (2019).
 - [22] R. V. Krems, “Cold controlled chemistry,” *Physical Chemistry Chemical Physics* **10**, 4079 (2008).
 - [23] K.-K. K. Ni, S. Ospelkaus, D. Wang, G. Quémener, B. Neyenhuis, M. H.G. G. De Miranda, J. L. Bohn, J. Ye, and D. S. Jin, “Dipolar collisions of polar molecules in the quantum regime,” *Nature* **464**, 1324–1328 (2010).
 - [24] Xin Ye, Mingyang Guo, Maykel L. González-Martínez, Goulven Quémener, and Dajun Wang, “Collisions of ultracold $^{23}\text{Na}^{87}\text{Rb}$ molecules with controlled chemical reactivities,” *Science Advances* **4**, eaaq0083 (2018).
 - [25] S. Ospelkaus, K-K K. Ni, D. Wang, M. H.G. G de Miranda, B. Neyenhuis, G. Quémener, P. S. Julienne, J. L. Bohn, D. S. Jin, and J. Ye, “Quantum-state controlled chemical reactions of ultracold potassium-rubidium molecules,” *Science* **327**, 853 (2010).
 - [26] D. DeMille, “Quantum computation with trapped polar molecules,” *Physical Review Letters* **88**, 067901 (2002).
 - [27] S. F. Yelin, K. Kirby, and Robin Côté, “Schemes for robust quantum computation with polar molecules,” *Physical Review A* **74**, 050301(R) (2006).
 - [28] Phelan Yu, Lawrence W. Cheuk, Ivan Kozyryev, and John M. Doyle, “A scalable quantum computing platform using symmetric-top molecules,” *New Journal of Physics* **21**, 093049 (2019).
 - [29] Lincoln D Carr, David DeMille, Roman V Krems, and Jun Ye, “Cold and ultracold molecules: science, technology and applications,” *New Journal of Physics* **11**, 055049 (2009).
 - [30] A. Micheli, G. K. Brennen, and P. Zoller, “A toolbox for lattice-spin models with polar molecules,” *Nature Physics* **2**, 341–347 (2006).
 - [31] Yicheng Bao, Scarlett S. Yu, Loïc Anderegg, Eunmi Chae, Wolfgang Ketterle, Kang-Kuen Ni, and John M. Doyle, “Dipolar spin-exchange and entanglement between molecules in an optical tweezer array,” [arXiv:2211.09780](https://arxiv.org/abs/2211.09780) (2022), [10.48550/arXiv.2211.09780](https://arxiv.org/abs/2211.09780), [arXiv:2211.09780](https://arxiv.org/abs/2211.09780) [physics, physics:quant-ph] type: article.
 - [32] Connor M. Holland, Yukai Lu, and Lawrence W. Cheuk, “On-Demand Entanglement of Molecules in a Reconfigurable Optical Tweezer Array,” [arXiv:2210.06309](https://arxiv.org/abs/2210.06309) (2022), [10.48550/arXiv.2210.06309](https://arxiv.org/abs/2210.06309), [arXiv:2210.06309](https://arxiv.org/abs/2210.06309) [cond-mat, physics:physics, physics:quant-ph] type: article.
 - [33] Jeremy M. Sage, Sunil Sainis, Thomas Bergeman, and David DeMille, “Optical production of ultracold polar molecules,” *Physical Review Letters* **94**, 203001 (2005).
 - [34] K-K Ni, S Ospelkaus, M H G de Miranda, A Pe’er, B Neyenhuis, J J Zirbel, S Kotochigova, P S Julienne, D S Jin, and J Ye, “A high phase-space-density gas of polar molecules,” *Science* **322**, 231 (2008).
 - [35] Johann G. Danzl, Manfred J. Mark, Elmar Haller, Mattias Gustavsson, Russell Hart, Jesus Aldegunde, Jeremy M. Hutson, and Hanns Christoph Nägerl, “An ultracold high-density sample of rovibronic ground-state molecules in an optical lattice,” *Nature Physics* **6**, 265–270 (2010).
 - [36] K. Aikawa, D. Akamatsu, M. Hayashi, K. Oasa, J. Kobayashi, P. Naidon, T. Kishimoto, M. Ueda, and S. Inouye, “Coherent transfer of photoassociated molecules into the rovibrational ground state,” *Physical Review Letters* **105**, 203001 (2010).
 - [37] Tetsu Takekoshi, Lukas Reichsöllner, Andreas Schindewolf, Jeremy M. Hutson, C. Ruth Le Sueur, Olivier Dulieu, Francesca Ferlaino, Rudolf Grimm, and Hanns Christoph Nägerl, “Ultracold dense samples of dipolar rbc molecules in the rovibrational and hyperfine ground state,” *Physical Review Letters* **113**, 205301 (2014).
 - [38] Peter K. Molony, Philip D. Gregory, Zhonghua Ji, Bo Lu, Michael P. Köppinger, C. Ruth Le Sueur, Caroline L. Blackley, Jeremy M. Hutson, and Simon L. Cornish, “Creation of ultracold $\text{Rb } 87 \text{ cs } 133$ molecules in the rovibrational ground state,” *Physical Review Letters* **113**, 255301 (2014).
 - [39] Jee Woo Park, Sebastian A. Will, and Martin W. Zwierlein, “Ultracold dipolar gas of fermionic $\text{Na}^{23}\text{K}^{40}$

- molecules in their absolute ground state,” *Physical Review Letters* **114**, 205302 (2015).
- [40] Mingyang Guo, Bing Zhu, Bo Lu, Xin Ye, Fudong Wang, Romain Vexiau, Nadia Bouloufa-Maafa, Goulven Quémener, Olivier Dulieu, and Dajun Wang, “Creation of an ultracold gas of ground-state dipolar ^{23}Rb 87 molecules,” *Physical Review Letters* **116**, 205303 (2016).
 - [41] L. R. Liu, J. D. Hood, Y. Yu, J. T. Zhang, N. R. Hutzler, T. Rosenband, and K.-K. Ni, “Building one molecule from a reservoir of two atoms,” *Science* **360**, 900 (2018).
 - [42] Luigi De Marco, Giacomo Valtolina, Kyle Matsuda, William G. Tobias, Jacob P. Covey, and Jun Ye, “A degenerate fermi gas of polar molecules,” *Science* **363**, 853–856 (2019).
 - [43] M. D. Di Rosa, “Laser-cooling molecules,” *The European Physical Journal D* **31**, 395–402 (2004).
 - [44] Daniel McCarron, “Laser cooling and trapping molecules,” *Journal of Physics B: Atomic, Molecular and Optical Physics* **51**, 212001 (2018).
 - [45] M. R. Tarbutt, “Laser cooling of molecules,” *Contemporary Physics* **59**, 356–376 (2018).
 - [46] N J Fitch and M R Tarbutt, “Laser cooled molecules,” *Advances In Atomic, Molecular, and Optical Physics*, 157–262 (2021).
 - [47] Tim Langen, Giacomo Valtolina, Dajun Wang, and Jun Ye, “Quantum state manipulation and science of ultracold molecules,” *ArXiv* (2023), 10.48550/arXiv.2305.13445.
 - [48] T. K. Langin and D. DeMille, “Toward improved loading, cooling, and trapping of molecules in magneto-optical traps,” *New Journal of Physics* **25**, 043005 (2023).
 - [49] J. T. Bahns, W. C. Stwalley, and P. L. Gould, “Laser cooling of molecules: A sequential scheme for rotation, translation, and vibration,” *Journal of Chemical Physics* **104**, 9689 (1996).
 - [50] Huagang Xiao, Quan Shun Yang, Jun Zhu, and Tao Gao, “Ab initio investigation on the low-lying electronic states of thallium bromide,” *Spectrochimica Acta Part A: Molecular and Biomolecular Spectroscopy* **246**, 118998 (2021).
 - [51] Yu Feng Gao and Tao Gao, “Laser cooling of bh and gaf: insights from an ab initio study,” *Physical Chemistry Chemical Physics* **17**, 10830–10837 (2015).
 - [52] Yufeng Gao and Tao Gao, “A theoretical study on low-lying electronic states and spectroscopic properties of ph,” *Spectrochimica Acta Part A: Molecular and Biomolecular Spectroscopy* **118**, 308–314 (2014).
 - [53] Huagang Xiao, Shikui Dong, and Tao Gao, “Electronic structure and laser cooling of liag and liau molecules,” *Chemical Physics Letters* **793**, 139407 (2022).
 - [54] Huagang Xiao, Ruijie Zhang, Hongyu Ma, and Tao Gao, “Spectroscopy and rovibrational cooling of auf and its cation,” *Spectrochimica Acta Part A: Molecular and Biomolecular Spectroscopy* **277**, 121279 (2022).
 - [55] Huagang Xiao, Jiangnan Wang, Ruijie Zhang, Na Shan, and Tao Gao, “The vibrational and hyperfine spectroscopy toward laser cooling $^{87}\text{Sr}^{35}\text{Cl}$,” *Spectrochimica Acta Part A: Molecular and Biomolecular Spectroscopy* **282**, 121679 (2022).
 - [56] Rong Yang, Bin Tang, and Tao Gao, “Ab initio study on the electronic states and laser cooling of alcl and albr,” *Chinese Physics B* **25**, 043101 (2016).
 - [57] Shuying Kang, Fangguang Kuang, Gang Jiang, and Jiguang Du, “The suitability of barium monofluoride for laser cooling from ab initio study,” *Molecular Physics* **114**, 810–818 (2016).
 - [58] Shuying Kang, Yufeng Gao, Fangguang Kuang, Tao Gao, Jiguang Du, and Gang Jiang, “Erratum: Theoretical study of laser cooling of magnesium monofluoride using ab initio methods,” *Physical Review A* **92**, 069902 (2015).
 - [59] Shuying Kang, Yufeng Gao, Fangguang Kuang, Tao Gao, Jiguang Du, and Gang Jiang, “Theoretical study of laser cooling of magnesium monofluoride using ab initio methods,” *Physical Review A - Atomic, Molecular, and Optical Physics* **91**, 042511 (2015).
 - [60] Kayla J. Rodriguez, Nickolas H. Pilgram, Daniel S. Barker, Stephen P. Eckel, and Eric B. Norrgard, “Simulations of a frequency-chirped magneto-optical trap of MgF ,” *ArXiv* (2023), 10.48550/arXiv.2305.04879, arXiv:2305.04879 [physics] type: article.
 - [61] R. L. Lambo, G. K. Koyanagi, A. Ragyanszki, M. Horbatsch, R. Fournier, and E. A. Hessels, “Calculation of the local environment of a barium monofluoride molecule in an argon matrix: A step towards using matrix-isolated BaF for determining the electron electric dipole moment,” *Molecular Physics* **121**, e2198044 (2023).
 - [62] A. Marsman, M. Horbatsch, and E. A. Hessels, “Deflection of barium monofluoride molecules using the bichromatic force: A density-matrix simulation,” *ArXiv* (2023), 10.48550/arXiv.2305.10641.
 - [63] N. El-Kork, A. AlMasri Alwan, N. Abu El Kher, J. As-saf, T. Ayari, E. Alhseinat, and M. Korek, “Laser cooling with intermediate state of spin-orbit coupling of LuF molecule,” *Scientific Reports* **13**, 7087 (2023).
 - [64] Rong Yang, Yufeng Gao, Bin Tang, and Tao Gao, “The ab initio study of laser cooling of bbr and bcl,” *Physical Chemistry Chemical Physics* **17**, 1900–1906 (2014).
 - [65] J. Lim, J. R. Almond, M.A. Trigatzis, J.A. Devlin, N.J. Fitch, B.E. Sauer, M.R. Tarbutt, and E.A. Hinds, “Laser Cooled YbF Molecules for Measuring the Electron’s Electric Dipole Moment,” *Physical Review Letters* **120**, 123201 (2018).
 - [66] G. Z. Iwata, R. L. McNally, and T. Zelevinsky, “High-resolution optical spectroscopy with a buffer-gas-cooled beam of bah molecules,” *Physical Review A* **96**, 022509 (2017).
 - [67] E. B. Norrgard, E. R. Edwards, D. J. McCarron, M. H. Steinecker, D. DeMille, Shah Saad Alam, S. K. Peck, N. S. Wadia, and L. R. Hunter, “Hyperfine structure of the $b\ 3\ \Pi_1$ state and predictions of optical cycling behavior in the $x \rightarrow b$ transition of tlf,” *Physical Review A* **95**, 062506 (2017).
 - [68] Benjamin K. Stuhl, Brian C. Sawyer, Dajun Wang, and Jun Ye, “Magneto-optical trap for polar molecules,” *Physical Review Letters* **101**, 243002 (2008).
 - [69] T. A. Isaev, S. Hoekstra, and R. Berger, “Laser-cooled raf as a promising candidate to measure molecular parity violation,” *Physical Review A* **82**, 052521 (2010).
 - [70] Liang Xu, Yanning Yin, Bin Wei, Yong Xia, and Jianping Yin, “Calculation of vibrational branching ratios and hyperfine structure of $^{24}\text{Mg}^{19}\text{F}$ and its suitability for laser cooling and magneto-optical trapping,” *Physical Review A* **93**, 013408 (2016).
 - [71] Eric Norrgard, Yuly Chamorro, Catherine Cook-

- sey, Stephen Eckel, Nickolas Pilgram, Kayla Rodriguez, Howard Yoon, Lukas Pasteka, and Anastasia Borschevsky, “Radiative Decay Rate and Branching Fractions of MgF,” *ArXiv* (2023), 10.48550/arXiv.2303.16276.
- [72] Tao Chen, Wenhao Bu, and Bo Yan, “Erratum: Structure, branching ratios, and a laser-cooling scheme for the baf 138 molecule,” *Physical Review A* **100**, 029901 (2019).
- [73] Qian Liang, Tao Chen, Wen Hao Bu, Yu He Zhang, and Bo Yan, “Laser cooling with adiabatic passage for type-ii transitions,” *Frontiers of Physics* **16**, 32501 (2021).
- [74] Wenhao Bu, Tao Chen, Guitao Lv, and Bo Yan, “Cold collision and high-resolution spectroscopy of buffer-gas-cooled baf molecules,” *Physical Review A* **95**, 032701 (2017).
- [75] Tao Chen, Wenhao Bu, and Bo Yan, “Structure, branching ratios, and a laser-cooling scheme for the ^{138}BaF molecule,” *Physical Review A* **94**, 063415 (2016).
- [76] Wenhao Bu, Yuhe Zhang, Qian Liang, Tao Chen, and Bo Yan, “Saturated absorption spectroscopy of buffer-gas-cooled barium monofluoride molecules,” *Frontiers of Physics* **17**, 1–7 (2022).
- [77] Tao Chen, Wenhao Bu, and Bo Yan, “Radiative deflection of a baf molecular beam via optical cycling,” *Physical Review A* **96**, 053401 (2017).
- [78] Ralf Albrecht, Michael Scharwaechter, Tobias Sixt, Lucas Hofer, and Tim Langen, “Buffer-gas cooling, high-resolution spectroscopy, and optical cycling of barium monofluoride molecules,” *Physical Review A* **101**, 013413 (2020).
- [79] Felix Kogel, Marian Rockenhäuser, Ralf Albrecht, and Tim Langen, “A laser cooling scheme for precision measurements using fermionic barium monofluoride ($^{137}\text{Ba}^{19}\text{F}$) molecules,” *New Journal of Physics* **23**, 095003 (2021).
- [80] Yuhe Zhang, Zixuan Zeng, Qian Liang, Wenhao Bu, and Bo Yan, “Doppler cooling of buffer-gas-cooled barium monofluoride molecules,” *Physical Review A* **105**, 033307 (2022).
- [81] Marian Rockenhäuser, Felix Kogel, Einus Pultinevičius, and Tim Langen, “Absorption spectroscopy for laser cooling and high-fidelity detection of barium monofluoride molecules,” *ArXiv* (2023), 10.48550/arXiv.2307.08312.
- [82] S. Truppe, S. Marx, S. Kray, M. Doppelbauer, S. Hofsäss, H. C. Schewe, N. Walter, J. Pérez-Riós, B. G. Sartakov, and G. Meijer, “Spectroscopic characterization of aluminum monofluoride with relevance to laser cooling and trapping,” *Physical Review A* **100**, 052513 (2019).
- [83] Maximilian Doppelbauer, Nicole Walter, Simon Hofsäss, Silvio Marx, H. Christian Schewe, Sebastian Kray, Jesús Pérez-Riós, Boris G. Sartakov, Stefan Truppe, and Gerard Meijer, “Characterisation of the $b^3\sigma^+, v = 0$ state and its interaction with the $a^1\pi$ state in aluminium monofluoride,” *Molecular Physics* **119**, e1810351 (2021).
- [84] J. C. Schnaubelt, J. C. Shaw, and D. J. McCarron, “Cold ch radicals for laser cooling and trapping,” *arXiv:2109.03953* (2021).
- [85] Rees L. McNally, Ivan Kozyryev, Sebastian Vazquez-Carson, Konrad Wenz, Tianli Wang, and Tanya Zelevinsky, “Optical cycling, radiative deflection and laser cooling of barium monohydride (^{138}BaH),” *New Journal of Physics* **22**, 083047 (2020).
- [86] M. G. Tarallo, G. Z. Iwata, and T. Zelevinsky, “Bah molecular spectroscopy with relevance to laser cooling,” *Physical Review A* **93**, 032509 (2016).
- [87] Timur A. Isaev and Robert Berger, “Polyatomic candidates for cooling of molecules with lasers from simple theoretical concepts,” *Physical Review Letters* **116**, 063006 (2016).
- [88] Ivan Kozyryev, Louis Baum, Kyle Matsuda, Boerge Hemmerling, and John M. Doyle, “Radiation pressure force from optical cycling on a polyatomic molecule,” *Journal of Physics B: Atomic, Molecular and Optical Physics* **49**, 134002 (2016).
- [89] Ivan Kozyryev, Louis Baum, Kyle Matsuda, and John M. Doyle, “Proposal for laser cooling of complex polyatomic molecules,” *ChemPhysChem* **17**, 3641–3648 (2016).
- [90] Louis Baum, Nathaniel B. Vilas, Christian Hallas, Benjamin L. Augenbraun, Shivam Raval, Debayan Mitra, and John M. Doyle, “1d magneto-optical trap of polyatomic molecules,” *Physical Review Letters* **124**, 133201 (2020).
- [91] Benjamin L. Augenbraun, Alexander Frenett, Hiromitsu Sawaoka, Christian Hallas, Nathaniel B. Vilas, Abdullah Nasir, Zack D. Lasner, and John M. Doyle, “Zeeman-sisyphus deceleration of molecular beams,” *Physical Review Letters* , 263002 (2021).
- [92] Debayan Mitra, Nathaniel B. Vilas, Christian Hallas, Loïc Anderegg, Benjamin L. Augenbraun, Louis Baum, Calder Miller, Shivam Raval, and John M. Doyle, “Direct laser cooling of a symmetric top molecule,” *Science* **369**, 1366–1369 (2020).
- [93] Nathaniel B. Vilas, Christian Hallas, Loïc Anderegg, Paige Robichaud, Andrew Winnicki, Debayan Mitra, and John M. Doyle, “Magneto-optical trapping and sub-Doppler cooling of a polyatomic molecule,” *Nature* **606**, 70–74 (2022).
- [94] Ivan Kozyryev, Louis Baum, Kyle Matsuda, Benjamin L. Augenbraun, Loïc Anderegg, Alexander P. Sedlack, and John M. Doyle, “Sisyphus laser cooling of a polyatomic molecule,” *Physical Review Letters* **118**, 173201 (2017).
- [95] Benjamin L. Augenbraun, Zack D. Lasner, Alexander Frenett, Hiromitsu Sawaoka, Calder Miller, Timothy C. Steimle, and John M. Doyle, “Laser-cooled polyatomic molecules for improved electron electric dipole moment searches,” *New Journal of Physics* **22**, 22003 (2020).
- [96] Benjamin L. Augenbraun, Loïc Anderegg, Christian Hallas, Zack D. Lasner, Nathaniel B. Vilas, and John M. Doyle, “Direct Laser Cooling of Polyatomic Molecules,” *ArXiv* (2023), 10.48550/arXiv.2302.10161.
- [97] J. F. Barry, D. J. McCarron, E. B. Norrgard, M. H. Steinecker, and D. DeMille, “Magneto-optical trapping of a diatomic molecule,” *Nature* **512**, 286–289 (2014).
- [98] D. J. McCarron, M. H. Steinecker, Y. Zhu, and D. DeMille, “Magnetic trapping of an ultracold gas of polar molecules,” *Phys. Rev. Lett.* **121**, 13202 (2018).
- [99] Loïc Anderegg, Benjamin L. Augenbraun, Eunmi Chae, Boerge Hemmerling, Nicholas R. Hutzler, Aakash Ravi, Alejandra Collopy, Jun Ye, Wolfgang Ketterle, and John M. Doyle, “Radio frequency magneto-optical trapping of caf with high density,” *Physical Review Letters*

- [119, 103201 \(2017\)](#).
- [100] S. Truppe, H. J. Williams, M. Hambach, L. Caldwell, N. J. Fitch, E. A. Hinds, B. E. Sauer, and M. R. Tarbutt, "Molecules cooled below the doppler limit," *Nature Physics* **13**, 1173–1176 (2017).
 - [101] H J Williams, S Truppe, M Hambach, L Caldwell, N J Fitch, E A Hinds, B E Sauer, and M R Tarbutt, "Characteristics of a magneto-optical trap of molecules," *New Journal of Physics* **19**, 113035 (2017).
 - [102] Alejandra L. Collopy, Shiqian Ding, Yewei Wu, Ian A. Finneran, Loïc Anderegg, Benjamin L. Augenbraun, John M. Doyle, and Jun Ye, "3d magneto-optical trap of yttrium monoxide," *Physical Review Letters* **121**, 213201 (2018).
 - [103] N. B. Clayburn, T. H. Wright, E. B. Norrgard, D. DeMille, and L. R. Hunter, "Measurement of the molecular dipole moment and the hyperfine and Λ -doublet splittings of the $B^3\pi$ state of thallium fluoride," *Physical Review A* **102**, 052802 (2020).
 - [104] O. Grasdijk, O. Timgren, J. Kastelic, T. Wright, S. Lamoreaux, D. DeMille, K. Wenz, M. Aitken, T. Zelevinsky, T. Winick, and D. Kowall, "CeNTREX: a new search for time-reversal symmetry violation in the ^{205}Tl nucleus," *Quantum Science and Technology* **6**, 044007 (2021).
 - [105] Mingjie Wan, Di Yuan, Chengguo Jin, Fanhou Wang, Yujie Yang, You Yu, and Juxiang Shao, "Laser cooling of the AlCl molecule with a three-electronic-level theoretical model," *The Journal of Chemical Physics* **145**, 024309 (2016).
 - [106] J. R. Daniel, C. Wang, K. Rodriguez, T. Lewis, A. Teplukhin, B. Kendrick, C. Bardeen, and B. Hemmerling, "Spectroscopy on the $x^1\sigma^+ - a^1\pi$ transition of buffer-gas cooled AlCl ," *Physical Review A* **104**, 012801 (2021).
 - [107] Donald F. Rogowski and Arthur Fontijn, "The radiative lifetime of AlCl a $^1\Pi$," *Chemical Physics Letters* **137**, 219–222 (1987).
 - [108] Stephen R. Langhoff, Charles W. Bauschlicher, and Peter R. Taylor, "Theoretical studies of AlF , AlCl , and AlBr ," *The Journal of Chemical Physics* **88**, 5715–5725 (1988).
 - [109] Xiao Ying Ren, Zhi Yu Xiao, Yong Liu, and Bing Yan, "Configuration interaction study on the low-lying states of AlCl molecule," *Chinese Physics B* **30**, 053101 (2021).
 - [110] J. Mes, E. J. van Duijn, R. Zinkstok, S. Witte, and W. Hogervorst, "Third-harmonic generation of a continuous-wave Ti:Sapphire laser in external resonant cavities," *Applied Physics Letters* **82**, 4423–4425 (2003).
 - [111] Vasilij Ostroumov and Wolf Seelert, "1 w of 261 nm cw generation in a $\text{pr}^{3+}:\text{LiF}$ laser pumped by an optically pumped semiconductor laser at 479 nm," *Solid State Lasers XVII: Technology and Devices* **6871**, 68711K (2008).
 - [112] Z. Burkley, A. D. Brandt, C. Rasor, S. F. Cooper, and D. C. Yost, "Highly coherent, watt-level deep-uv radiation via a frequency-quadrupled Yb -fiber laser system," *Applied Optics* , 1657–1661 (2019).
 - [113] Zakary Burkley, Lucas de Sousa Borges, Ben Ohayon, Artem Golovizin, Jesse Zhang, and Paolo Crivelli, "Stable high power deep-uv enhancement cavity in ultra-high vacuum with fluoride coatings," *Optics Express* **29**, 27450–27459 (2021).
 - [114] D. J. McCarron, J. C. Shaw, and S. Hannig, "Stable 2 w continuous-wave 261.5 nm laser for cooling and trapping aluminum monochloride," *Optics Express* **29**, 37140–37149 (2021).
 - [115] W Jevons, "Spectroscopic investigations in connection with the active modification of nitrogen. iii.—spectra developed by the tetrachlorides of silicon and titanium," *Proceedings of the Royal Society of London. Series A, Containing Papers of a Mathematical and Physical Character* **89**, 187–193 (1913).
 - [116] W Jevons, "On the band-spectra of silicon oxide and chloride, and chlorides of carbon, boron, and aluminium," *Proceedings of the Royal Society of London. Series A, Containing Papers of a Mathematical and Physical Character* **106**, 174–194 (1924).
 - [117] B. N. Bhaduri and Alfred Fowler, "Band spectrum of aluminium chloride (AlCl)," *Proceedings of the Royal Society of London A* **145**, 321–336 (1934).
 - [118] W. Holst, "Über die rotationsstruktur der AlCl -banden," *Zeitschrift für Physik* **93**, 55–64 (1935).
 - [119] P. C. Mahanti, "Das bandenspektrum des aluminiumchlorids," *Zeitschrift für Physik* **88**, 550–558 (1934).
 - [120] E Miescher, "Absorptionsspektren und lebensdauer zweiatomiger moleküle mit freien valenzen," *Helvetica Physica Acta* **9**, 693 (1936).
 - [121] Devendra Sharma, "Two new band systems of the AlCl molecule," *The Astrophysical Journal* **113**, 210 (1951).
 - [122] R. F. Barrow, "Maxima in the Potential Energy-Distance Functions of Diatomic Molecules," *The Journal of Chemical Physics* **22**, 573–573 (1954).
 - [123] S. Paddi Reddy and P. Tiruvenganna Rao, "The emission spectrum of aluminum monochloride in the vacuum ultraviolet," *Canadian Journal of Physics* **35**, 912–917 (1957).
 - [124] R. F. Barrow, "Dissociation energies of the gaseous mono-halides of boron, aluminium, gallium, indium and thallium," *Transactions of the Faraday Society* **56**, 952 (1960).
 - [125] David R. Lide, "High-temperature microwave spectroscopy : AlF and AlCl ," *The Journal of Chemical Physics* **42**, 1013–1018 (1965).
 - [126] David R. Lide, "Erratum: "High-Temperature Microwave Spectroscopy: AlF and AlCl ,"," *The Journal of Chemical Physics* **46**, 1224–1224 (1967).
 - [127] F. C. Wyse and Walter Gordy, "Millimeter wave rotational spectra of AlCl , AlBr , and AlI ," *The Journal of Chemical Physics* **56**, 2130–2136 (1972).
 - [128] J. Hoeft, T. Törring, and E. Tiemann, "Hyperfeinstruktur von AlCl und AlBr / hyperfine structure of AlCl and AlBr ," *Zeitschrift für Naturforschung A* **28**, 1066–1068 (1973).
 - [129] Frank J. Lovas and Eberhard Tiemann, "Microwave Spectral Tables I. Diatomic Molecules," *Journal of Physical and Chemical Reference Data* **3**, 609–770 (1974).
 - [130] Hg Schnöckel, "Infrarotabsorption von AlCl und AlBr in festen edelgasmatrizen," *Zeitschrift für Naturforschung B* **31**, 1291–1292 (1976).
 - [131] Kin Ichi Tsunoda, Kitao Fujiwara, and Keiichiro Fuwa, "Determination of chlorine and bromine by molecular absorption of aluminum monohalides at high temperature," *Analytical Chemistry* **50**, 861–865 (1978).

- [132] Ram Samujh Ram, S B Rai, K N Upadhyaya, and D K Rai, "The $a^1\pi-x^1\sigma^+$, $a^3\pi-x^1\sigma^+$, and $b^3\sigma^+-a^3\pi$ systems of alcl ," *Physica Scripta* **26**, 383–397 (1982).
- [133] E. Mahieu, I. Dubois, and H. Bredohl, "The $a^1\Pi-x^1\Sigma^+$ transition of alcl ," *Journal of Molecular Spectroscopy* **134**, 317–328 (1989).
- [134] E. Mahieu, I. Dubois, and H. Bredohl, "The triplet states of alcl ," *Journal of Molecular Spectroscopy* **138**, 264–271 (1989).
- [135] David V. Dearden, Russell D. Johnson, and Jeffrey W. Hudgens, "Aluminum monochloride excited states observed by resonance-enhanced multiphoton ionization spectroscopy," *The Journal of Chemical Physics* **99**, 7521–7528 (1993).
- [136] J. F. Ogilvie and S. C. Liao, "The inversion of spectral data of alcl and $\text{sis } x^1\sigma^+$," *Acta Physica Hungarica* **74**, 365–377 (1994).
- [137] H. G. Hedderich, M. Dulick, and P. F. Bernath, "High resolution emission spectroscopy of alcl at 20μ ," *The Journal of Chemical Physics* **99**, 8363–8370 (1993).
- [138] Kristine D. Hensel, Christian Styger, Wolfgang Jäger, A. J. Merer, and M. C.L. L. Gerry, "Microwave spectra of metal chlorides produced using laser ablation," *The Journal of Chemical Physics* **99**, 3320–3328 (1993).
- [139] M.D. Saksena, V.S. Dixit, and Mahavir Singh, "Rotational analysis of the 0–0 band of the $a^3\Pi-x^1\Sigma^+$ transition of alcl ," *Journal of Molecular Spectroscopy* **187**, 1–5 (1998).
- [140] Pekka Parvinen and Lauri H.J. Lajunen, "The zeeman splitting of aluminium monochloride molecular absorption bands as the possible interference in atomic absorption spectrometry," *Spectroscopy Letters* **31**, 1761–1769 (1998).
- [141] V. Brites, D. Hammoutene, and M. Hochlaf, "Spectroscopy, metastability, and single and double ionization of alcl ," *The Journal of Physical Chemistry A* **112**, 13419–13426 (2008).
- [142] Mama Pamboundom, Théophile Tchakoua, and Mama Nsangou, "Rotational excitation of alcl induced by its collision with helium: cross sections and collisional rate coefficients," *Astrophysics and Space Science* **361**, 150 (2016).
- [143] Alex Preston, Sean Jackson, and Richard Mawhorter, "Global rovibrational fits for AlCl , BiCl , and BiF : Benchmarks for novel physics," *Chemical Physics Letters* **807**, 140089 (2022).
- [144] Stephen R. Langhoff, Charles W. Bauschlicher, and Peter R. Taylor, "Erratum: Theoretical studies of AlF , AlCl , and AlBr [*J. Chem. Phys.* 88, 5715 (1988)]," *The Journal of Chemical Physics* **89**, 7650–7650 (1988).
- [145] C M Andreazza, A A de Almeida, and R M Vichiatti, "Formation of alcl by radiative association," *Monthly Notices of the Royal Astronomical Society* **477**, 548–551 (2018).
- [146] Mahdi Yousefi and Peter F. Bernath, "Line lists for alf and alcl in the $x^1\Sigma^+$ ground state," *The Astrophysical Journal Supplement Series* **237**, 8 (2018).
- [147] Antoine Aerts and Alex Brown, "A revised nuclear quadrupole moment for aluminum: Theoretical nuclear quadrupole coupling constants of aluminum compounds," *The Journal of Chemical Physics* **150**, 224302 (2019).
- [148] Jian Gang Xu, Cong Ying Zhang, and Yun Guang Zhang, "Vibronic spectra of aluminium monochloride relevant to circumstellar molecule," *Chinese Physics B* **29**, 033102 (2020).
- [149] Jinping Zhang, Hui Li, and Yanqin Ma, "Rovibrational properties of the $a^1\pi-x^1\sigma^+$ system of the alcl radical," *Computational and Theoretical Chemistry* **1202**, 113307 (2021).
- [150] Zhi Qin, Tianrui Bai, and Linhua Liu, "Temperature-dependent direct photodissociation cross sections and rates of alcl ," *Monthly Notices of the Royal Astronomical Society* **508**, 2848–2854 (2021).
- [151] R. Bala, V. S. Prasanna, D. Chakravarti, D. Mukherjee, and B. P. Das, "Ab initio spectroscopic studies of alf and alcl molecules," *ArXiv* (2023), 10.48550/arXiv.2303.08681.
- [152] Savinder Kaur, Anand Bharadvaja, and K. L. Baluja, "Low to high energy electron interactions with AlCl ," *The European Physical Journal D* **77**, 142 (2023).
- [153] J Cernicharo and M Guelin, "Metals in $\text{irc} +10216$: detection of nacl , alcl , and kcl , and tentative detection of alf ," *Astronomy and Astrophysics* **183**, L10–L12 (1987).
- [154] K. E. Saavik Ford, David A. Neufeld, Peter Schilke, and Gary J. Melnick, "Detection of formaldehyde toward the extreme carbon star $\text{irc} +10216$," *The Astrophysical Journal* **614**, 990–1006 (2004).
- [155] M. Agúndez, J. P. Fonfría, J. Cernicharo, C. Kahane, F. Daniel, and M. Guélin, "Molecular abundances in the inner layers of $\text{irc} +10216$," *Astronomy and Astrophysics* **543**, A48 (2012).
- [156] T. Kamiński, K. T. Wong, M. R. Schmidt, H. S.P. Müller, C. A. Gottlieb, I. Cherchneff, K. M. Menten, D. Keller, S. Brünken, J. M. Winters, and N. A. Patel, "An observational study of dust nucleation in mira (o ceti): I. variable features of alo and other al -bearing species," *Astronomy and Astrophysics* **592**, 42 (2016).
- [157] L. Decin, A. M. S. Richards, L. B. F. M. Waters, T. Danilovich, D. Gobrecht, T. Khouri, W. Homan, J. M. Bakker, M. Van de Sande, J. A. Nuth, and E. De Beck, "Study of the aluminium content in agb winds using alma - indications for the presence of gas-phase $(\text{al}_2\text{o}_3)_n$ clusters," *Astronomy and Astrophysics* **608**, A55 (2017).
- [158] Peter F. Bernath, "MoLLIST: Molecular Line Lists, Intensities and Spectra," *Journal of Quantitative Spectroscopy and Radiative Transfer* **240**, 106687 (2020).
- [159] Sergei N Yurchenko, Emma Nogué, Ala'a A A Az-zam, and Jonathan Tennyson, "ExoMol line lists – XLVII. Rovibronic spectrum of aluminium monochloride (AlCl)," *Monthly Notices of the Royal Astronomical Society* **520**, 5183–5191 (2023).
- [160] Jonathan Tennyson, Sergei N. Yurchenko, Ahmed F. Al-Refaie, Victoria H.J. Clark, Katy L. Chubb, Eamon K. Conway, Akhil Dewan, Maire N. Gorman, Christian Hill, A. E. Lynas-Gray, Thomas Mellor, Laura K. McKemmish, Alec Owens, Oleg L. Polyansky, Mikhail Semenov, Wilfrid Somogyi, Giovanna Tinetti, Apoorva Upadhyay, Ingo Waldmann, Yixin Wang, Samuel Wright, and Olga P. Yurchenko, "The 2020 release of the exomol database: Molecular line lists for exoplanet and other hot atmospheres," *Journal of Quantitative Spectroscopy and Radiative Transfer* **255**, 107228 (2020).
- [161] Yixin Wang, Jonathan Tennyson, and Sergei Yurchenko, "Empirical line lists in the exomol database," *Atoms* **8**, 7 (2020).

- [162] Kouji Yasuda, Kunio Saegusa, and Toru H. Okabe, “New method for production of solar-grade silicon by subhalide reduction,” *Materials Transactions* **50**, 2873–2878 (2009).
- [163] Kouji Yasuda, Kunio Saegusa, and Toru H. Okabe, “Production of solar-grade silicon by halidothermic reduction of silicon tetrachloride,” *Metallurgical and Materials Transactions B: Process Metallurgy and Materials Processing Science* **42**, 37–49 (2011).
- [164] Kouji Yasuda, Kunio Saegusa, and Toru H. Okabe, “Aluminum subhalide as a reductant for metallothermic reduction,” *High Temperature Materials and Processes* **30**, 411–423 (2011).
- [165] W. K. McGregor, J. A. Drakes, K. S. Beale, and F. G. Sherrell, “The alcl absorption feature in solid rocket plume radiation,” (American Institute of Aeronautics and Astronautics Inc, AIAA, 1992).
- [166] W. K. McGregor, J. A. Drakes, K. S. Beale, F. G. Sherrell, W. K. McGregor, J. A. Drakes, K. S. Beale, and F. G. Sherrell, “Alcl absorption feature in solid rocket plume radiation,” *JTHT* **7**, 736–739 (1993).
- [167] S. M. Oliver, W. K. McGregor, R. A. Reed, J. A. Drakes, and K. Beale, “Analysis of the alcl absorption feature and the searchlight emission effect observed in solid-propellant rocket plumes,” *Arnold Engineering Development Center* (1992).
- [168] Pekka Parvinen and Lauri H.J. Lajunen, “Determination of chloride in drinking and ground water by alcl molecular absorption spectrometry using graphite furnace atomic absorption spectrometer,” *Talanta* **50**, 67–71 (1999).
- [169] Matthias Tacke and Hansgeorg Schnöckel, “Metastable alcl as a solid and in solution,” *Inorganic Chemistry* **28**, 2895–2896 (1989).
- [170] Jamie C. Shaw, *Prospects for laser cooling and trapping aluminum monochloride*, Ph.D. thesis, University of Connecticut (2022).
- [171] Nicholas R. Hutzler, Hsin-I I. Lu, and John M. Doyle, “The buffer gas beam: An intense, cold, and slow source for atoms and molecules,” *Chemical Reviews* **112**, 4803–4827 (2012).
- [172] J. F. Barry, E. S. Shuman, and D. DeMille, “A bright, slow cryogenic molecular beam source for free radicals,” *Physical Chemistry Chemical Physics* **13**, 18936–18947 (2011).
- [173] Taylor N. Lewis, Chen Wang, John R. Daniel, Madhav Dhital, Christopher J. Bardeen, and Boerge Hemmerling, “Optimizing pulsed-laser ablation production of alcl molecules for laser cooling,” *Physical Chemistry Chemical Physics* **23**, 22785 (2021).
- [174] J. C. Shaw and D. J. McCarron, “Bright, continuous beams of cold free radicals,” *Physical Review A* **102**, 041302 (2020).
- [175] John Michael Brown and Alan Carrington, *Rotational Spectroscopy of Diatomic Molecules* (Cambridge University Press, 2003).
- [176] R. E. Alonso, A. Svane, C. O. Rodríguez, and N. E. Christensen, “Nuclear quadrupole moment determination of ^{35}Cl , ^{79}Br , and ^{127}I ,” *Physical Review B* **69**, 125101 (2004).
- [177] John F. Barry, *Laser cooling and slowing of a diatomic molecule*, Ph.D. thesis, Yale University (2013).
- [178] M. R. Tarbutt and T. C. Steimle, “Modeling magneto-optical trapping of caF molecules,” *Physical Review A* **92**, 053401 (2021).
- [179] Matthew T. Hummon, Mark Yeo, Benjamin K. Stuhl, Alejandra L. Collopy, Yong Xia, and Jun Ye, “2d magneto-optical trapping of diatomic molecules,” *Physical Review Letters* **110**, 143001 (2013).
- [180] E. B. Norrgard, D. J. McCarron, M. H. Steinecker, M. R. Tarbutt, and D. DeMille, “Submillikelvin dipolar molecules in a radio-frequency magneto-optical trap,” *Physical Review Letters* **116**, 063004 (2016).
- [181] J. A. Devlin and M. R. Tarbutt, “Three-dimensional doppler, polarization-gradient, and magneto-optical forces for atoms and molecules with dark states,” *New Journal of Physics* **18**, 123017 (2016).
- [182] Xinye Xu, Thomas H. Loftus, John L. Hall, Alan Gallagher, and Jun Ye, “Cooling and trapping of atomic strontium,” *Journal of the Optical Society of America B* **20**, 968–976 (2003).
- [183] P. Kaebert, M. Stepanova, T. Poll, M. Petzold, S. Xu, M. Siercke, and S. Ospelkaus, “Characterizing the Zeeman slowing force for $^{40}\text{Ca}^{19}\text{F}$ molecules,” *New Journal of Physics* **23**, 093013 (2021).
- [184] D. Haubrich, H. Schadwinkel, F. Strauch, B. Ueberholz, R. Wynands, and D. Meschede, “Observation of individual neutral atoms in magnetic and magneto-optical traps,” *Europhysics Letters* **34**, 663 (1996).
- [185] P. A. Willems, R. A. Boyd, J. L. Bliss, and K. G. Libbrecht, “Stability of Magneto-optical Traps with Large Field Gradients: Limits on the Tight Confinement of Single Atoms,” *Physical Review Letters* **78**, 1660–1663 (1997).
- [186] Seokchan Yoon, Youngwoon Choi, Sangbum Park, Wangxi Ji, Jai-Hyung Lee, and Kyungwon An, “Characteristics of single-atom trapping in a magneto-optical trap with a high magnetic-field gradient,” *Journal of Physics: Conference Series* **80**, 012046 (2007).
- [187] M. Partlow, X. Miao, J. Bochmann, M. Cashen, and H. Metcalf, “Bichromatic slowing and collimation to make an intense helium beam,” *Physical Review Letters* **93**, 213004 (2004).
- [188] M. A. Chieda and E. E. Eyler, “Bichromatic slowing of metastable helium,” *Physical Review A* **86**, 053415 (2012).
- [189] Xiuxiu Yang, Chuanliang Li, Yanning Yin, Supeng Xu, Xingjia Li, Yong Xia, and Jianping Yin, “Bichromatic slowing of MgF molecules in multilevel systems,” *Journal of Physics B: Atomic, Molecular and Optical Physics* **50**, 015001 (2016).
- [190] Christopher Corder, Brian Arnold, and Harold Metcalf, “Laser Cooling without Spontaneous Emission,” *Physical Review Letters* **114**, 043002 (2015).
- [191] Ivan Kozyryev, Louis Baum, Leland Aldridge, Phelan Yu, Edward E. Eyler, and John M. Doyle, “Coherent Bichromatic Force Deflection of Molecules,” *Physical Review Letters* **120**, 063205 (2018).
- [192] S. E. Galica, L. Aldridge, D. J. McCarron, E. E. Eyler, and P. L. Gould, “Deflection of a molecular beam using the bichromatic stimulated force,” *Physical Review A* **98**, 023408 (2018).
- [193] James Greenberg, O. A. Krohn, Jason A. Bossert, Yomay Shyur, David Macaluso, N. J. Fitch, and H. J. Lewandowski, “Velocity-tunable beam of continuously decelerated polar molecules for cold ion-molecule reaction studies,” *Review of Scientific Instruments* **92**,

- 103202 (2021).
- [194] P. Aggarwal, H. L. Bethlem, A. Boeschoten, A. Borschevsky, K. Esajas, Y. Hao, S. Hoekstra, K. Jungmann, V. R. Marshall, T. B. Meijknecht, M. C. Mooij, R. G. E. Timmermans, A. Touwen, W. Ubachs, L. Willmann, Y. Yin, and A. Zapara, “A supersonic laser ablation beam source with narrow velocity spreads,” *Review of Scientific Instruments* **92**, 033202 (2021).
 - [195] Yomay Shyur, N. J. Fitch, Jason A. Bossert, Terry Brown, and H. J. Lewandowski, “A high-voltage amplifier for traveling-wave Stark deceleration,” *Review of Scientific Instruments* **89**, 084705 (2018).
 - [196] Yomay Shyur, Jason A. Bossert, and H. J. Lewandowski, “Pulsed operation of a ring Stark decelerator,” *Journal of Physics B: Atomic, Molecular and Optical Physics* **51**, 165101 (2018).
 - [197] Andreas Osterwalder, Samuel A. Meek, Georg Hammer, Henrik Haak, and Gerard Meijer, “Deceleration of neutral molecules in macroscopic traveling traps,” *Physical Review A* **81**, 051401 (2010).
 - [198] Samuel A. Meek, Maxwell F. Parsons, Georg Heyne, Viktor Platschkowski, Henrik Haak, Gerard Meijer, and Andreas Osterwalder, “A traveling wave decelerator for neutral polar molecules,” *Review of Scientific Instruments* **82**, 093108 (2011).
 - [199] J. E. van den Berg, S. C. Mathavan, C. Meinema, J. Nauta, T. H. Nijbroek, K. Jungmann, H. L. Bethlem, and S. Hoekstra, “Traveling-wave deceleration of SrF molecules,” *Journal of Molecular Spectroscopy Spectroscopic Tests of Fundamental Physics*, **300**, 22–25 (2014).
 - [200] J. C. Shaw, M. A. Semco, W. B. Wortley, and D. J. McCarron, “Optical cycling in alcl molecules,” (in preparation).
 - [201] L. R. Hunter, S. K. Peck, A. S. Greenspon, S. Saad Alam, and D. DeMille, “Prospects for laser cooling tlf,” *Physical Review A* **85**, 012511 (2012).
 - [202] R. J. Hendricks, D. A. Holland, S. Truppe, B. E. Sauer, and M. R. Tarbutt, “Vibrational branching ratios and hyperfine structure of 11bh and its suitability for laser cooling,” *Frontiers in Physics* **2**, 51 (2014).
 - [203] S. Hofsäss, M. Doppelbauer, S. C. Wright, S. Kray, B. G. Sartakov, J. Pérez-Ríos, G. Meijer, and S. Truppe, “Optical cycling of AlF molecules,” *New Journal of Physics* **23**, 075001 (2021).
 - [204] D. J. Berkeland and M. G. Boshier, “Destabilization of dark states and optical spectroscopy in Zeeman-degenerate atomic systems,” *Physical Review A* **65**, 033413 (2002).
 - [205] H. R. Gray, R. M. Whitley, and C. R. Stroud, “Coherent trapping of atomic populations,” *Optics Letters* **3**, 218–220 (1978).
 - [206] R. N. Shakhmuratov, J. Odeurs, R. Coussement, and A. Szabo, “Dark and bright states of the coherently excited three-level atom,” *Laser Physics* **1**, 39–50 (2004).
 - [207] J. F. Barry, E. S. Shuman, E. B. Norrgard, and D. DeMille, “Laser radiation pressure slowing of a molecular beam,” *Physical Review Letters* **108**, 103002 (2012).
 - [208] Boerge Hemmerling, Eunmi Chae, Aakash Ravi, Loic Anderegg, Garrett K Drayna, Nicholas R Hutzler, Alejandra L Collopy, Jun Ye, Wolfgang Ketterle, and John M Doyle, “Laser slowing of caf molecules to near the capture velocity of a molecular mot,” *Journal of Physics B: Atomic, Molecular and Optical Physics* **49**, 174001 (2016).
 - [209] Mark Yeo, Matthew T. Hummon, Alejandra L. Collopy, Bo Yan, Boerge Hemmerling, Eunmi Chae, John M. Doyle, and Jun Ye, “Rotational state microwave mixing for laser cooling of complex diatomic molecules,” *Physical Review Letters* **114**, 223003 (2015).
 - [210] Stephen Eckel, Daniel S. Barker, Eric B. Norrgard, and Julia Scherschligt, “PyLCP: A Python package for computing laser cooling physics,” *Computer Physics Communications* **270**, 108166 (2022).
 - [211] J. P. Gordon and A. Ashkin, “Motion of atoms in a radiation trap,” *Physical Review A* **21**, 1606–1617 (1980).
 - [212] P. J. Ungar, D. S. Weiss, E. Riis, and S. Shu, “Optical molasses and multilevel atoms: theory,” *Journal of the Optical Society of America B* **6**, 2058–2071 (1989).
 - [213] E. S. Shuman, J. F. Barry, D. R. Glenn, and D. DeMille, “Radiative force from optical cycling on a diatomic molecule,” *Physical Review Letters* **103**, 223001 (2009).
 - [214] Justin J. Bureau, Parul Aggarwal, Kameron Mehling, and Jun Ye, “Blue-Detuned Magneto-optical Trap of Molecules,” *Physical Review Letters* **130**, 193401 (2023).
 - [215] K.-A. Brickman, M.-S. Chang, M. Acton, A. Chew, D. Matsukevich, P. C. Haljan, V. S. Bagnato, and C. Monroe, “Magneto-optical trapping of cadmium,” *Physical Review A* **76**, 043411 (2007).
 - [216] W. Press, B. Flannery, S. Teukolsky, and W. Vetterling, *Numerical Recipes: The Art of Scientific Computing* (Cambridge University Press, Cambridge, 1986).
 - [217] G. Herzberg, *Spectra of Diatomic Molecules*, Molecular Spectra and Molecular Structure (Van Nostrand, 1950) pp. 392–393.
 - [218] Hsin-I Lu, Julia Rasmussen, Matthew J. Wright, Dave Patterson, and John M. Doyle, “A cold and slow molecular beam,” *Physical Chemistry Chemical Physics* **13**, 18986 (2011).
 - [219] Eunmi Chae, Loic Anderegg, Benjamin L Augenbraun, Aakash Ravi, Boerge Hemmerling, Nicholas R Hutzler, Alejandra L Collopy, Jun Ye, Wolfgang Ketterle, and John M Doyle, “One-dimensional magneto-optical compression of a cold caf molecular beam,” *New Journal of Physics* **19**, 033035 (2017).
 - [220] Supeng Xu, Meng Xia, Ruoxi Gu, Yanning Yin, Liang Xu, Yong Xia, and Jianping Yin, “Three-dimensional modeling of magneto-optical trapping of MgF molecules with multilevel rate equations,” *Physical Review A* **99**, 033408 (2019).
 - [221] S. Xu, P. Kaebert, M. Stepanova, T. Poll, M. Siercke, and S. Ospelkaus, “Maximizing the capture velocity of molecular magneto-optical traps with Bayesian optimization,” *New Journal of Physics* **23**, 063062 (2021).